nature

https://doi.org/10.1038/s41586-020-2700-3

Accelerated Article Preview

Sex differences in immune responses that underlie COVID-19 disease outcomes

Received: 4 June 2020

Accepted: 19 August 2020

Accelerated Article Preview Published online 26 August 2020

Cite this article as: Takahashi, T. et al. Sex differences in immune responses that underlie COVID-19 disease outcomes. *Nature* https://doi.org/10.1038/s41586-020-2700-3 (2020).

Takehiro Takahashi, Mallory K. Ellingson, Patrick Wong, Benjamin Israelow, Carolina Lucas, Jon Klein, Julio Silva, Tianyang Mao, Ji Eun Oh, Maria Tokuyama, Peiwen Lu, Arvind Venkataraman, Annsea Park, Feimei Liu, Amit Meir, Jonathan Sun, Eric Y. Wang, Arnau Casanovas-Massana, Anne L. Wyllie, Chantal B.F. Vogels, Rebecca Earnest, Sarah Lapidus, Isabel M. Ott, Adam J. Moore, Yale IMPACT research team, Albert Shaw, John B. Fournier, Camila D. Odio, Shelli Farhadian, Charles Dela Cruz, Nathan D. Grubaugh, Wade L. Schulz, Aaron M. Ring, Albert I. Ko, Saad B. Omer & Akiko Iwasaki

Article

Sex differences in immune responses that underlie COVID-19 disease outcomes

https://doi.org/10.1038/s41586-020-2700-3

Received: 4 June 2020

Accepted: 19 August 2020

Published online: 26 August 2020

Takehiro Takahashi[1,21], Mallory K. Ellingson[2,21], Patrick Wong[1,21], Benjamin Israelow[1,3,21], Carolina Lucas[1,21], Jon Klein[1,21], Julio Silva[1,21], Tianyang Mao[1,21], Ji Eun Oh[1], Maria Tokuyama[1], Peiwen Lu[1], Arvind Venkataraman[1], Annsea Park[1], Feimei Liu[1,4], Amit Meir[5], Jonathan Sun[6], Eric Y. Wang[1], Arnau Casanovas-Massana[2], Anne L. Wyllie[2], Chantal B.F. Vogels[2], Rebecca Earnest[2], Sarah Lapidus[2], Isabel M. Ott[2,7], Adam J. Moore[2], Yale IMPACT research team*, Albert Shaw[3], John B. Fournier[3], Camila D. Odio[3], Shelli Farhadian[3], Charles Dela Cruz[8], Nathan D. Grubaugh[2], Wade L. Schulz[9,10], Aaron M. Ring[1], Albert I. Ko[2], Saad B. Omer[2,3,11,12] & Akiko Iwasaki[1,13] ✉

A growing body of evidence indicates sex differences in the clinical outcomes of coronavirus disease 2019 (COVID-19)[1–5]. However, whether immune responses against SARS-CoV-2 differ between sexes, and whether such differences explain male susceptibility to COVID-19, is currently unknown. In this study, we examined sex differences in viral loads, SARS-CoV-2-specific antibody titers, plasma cytokines, as well as blood cell phenotyping in COVID-19 patients. By focusing our analysis on patients with moderate disease who had not received immunomodulatory medications, our results revealed that male patients had higher plasma levels of innate immune cytokines such as IL-8 and IL-18 along with more robust induction of non-classical monocytes. In contrast, female patients mounted significantly more robust T cell activation than male patients during SARS-CoV-2 infection, which was sustained in old age. Importantly, we found that a poor T cell response negatively correlated with patients' age and was associated with worse disease outcome in male patients, but not in female patients. Conversely, higher innate immune cytokines in female patients associated with worse disease progression, but not in male patients. These findings reveal a possible explanation underlying observed sex biases in COVID-19, and provide an important basis for the development of a sex-based approach to the treatment and care of men and women with COVID-19.

Severe acute respiratory syndrome coronavirus-2 (SARS-CoV-2) is the novel coronavirus first detected in Wuhan, China, in November 2019, that causes coronavirus disease 2019 (COVID-19)[6]. On March 11th 2020, the World Health Organization declared COVID-19 a pandemic[7]. A growing body of evidence reveals that male sex is a risk factor for a more severe disease, including death. Globally, ~60% of deaths from COVID-19 are reported in men[5], and a cohort study of 17 million adults in England reported a strong association between male sex and risk of death from COVID-19 (hazard ratio 1.59, 95% confidence interval 1.53-1.65)[8].

Past studies have demonstrated that sex has a significant impact on the outcome of infections and has been associated with underlying differences in immune response to infection[9,10]. For example, prevalence of hepatitis A and tuberculosis are significantly higher in men compared with women[11]. Viral loads are consistently higher in male patients with hepatitis C virus (HCV) and human immunodeficiency virus (HIV)[12,13]. Conversely, women mount a more robust immune response to vaccines[14]. These findings collectively suggest a more robust ability among women to control infectious agents. However, the mechanism by which SARS-CoV-2 causes more severe disease in male patients than in female patients remains unknown.

To elucidate the immune responses against SARS-CoV-2 infection in men and women, we performed detailed analysis on the sex differences in immune phenotype via the assessment of viral loads, SARS-CoV-2 specific antibody levels, plasma cytokines/chemokines, and blood cell phenotypes.

[1]Department of Immunobiology, Yale University School of Medicine, New Haven, CT, 06520, USA. [2]Department of Epidemiology of Microbial Diseases, Yale School of Public Health, New Haven, CT, 06520, USA. [3]Department of Medicine, Section of Infectious Diseases, Yale University School of Medicine, New Haven, CT, 06520, USA. [4]Department of Biomedical Engineering, Yale School of Engineering & Applied Science, New Haven, CT, 06511, USA. [5]Boyer Center for Molecular Medicine, Department of Microbial Pathogenesis, Yale University, New Haven, CT, 06510, USA. [6]Department of Comparative Medicine, Yale University School of Medicine, New Haven, CT, 06520, USA. [7]Department of Ecology and Evolutionary Biology, Yale University, New Haven, CT, 06520, USA. [8]Department of Medicine, Section of Pulmonary and Critical Care Medicine, Yale University School of Medicine, New Haven, CT, 06520, USA. [9]Department of Laboratory Medicine, Yale University School of Medicine, New Haven, CT, 06520, USA. [10]Center for Outcomes Research and Evaluation, Yale-New Haven Hospital, New Haven, CT, 06520, USA. [11]Yale Institute for Global Health, Yale University, New Haven, CT, 06520, USA. [12]Yale School of Nursing, Yale University, Orange, CT, 06477, USA. [13]Howard Hughes Medical Institute, Chevy Chase, MD, 20815, USA. [21]These authors contributed equally: Takehiro Takahashi, Mallory K. Ellingson, Patrick Wong, Benjamin Israelow, Carolina Lucas, Jon Klein, Julio Silva, Tianyang Mao. *A list of authors and their affiliations appears at the end of the paper. ✉e-mail: akiko.iwasaki@yale.edu

Overview of the study design

Patients who were admitted to the Yale-New Haven Hospital between March 18th and May 9th, 2020 and were confirmed positive for SARS-CoV-2 by RT–PCR from nasopharyngeal and/or oropharyngeal swabs in CLIA-certified laboratory were enrolled through the IMPACT biorepository study[15]. In this IMPACT study, biospecimens including blood, nasopharyngeal swabs, saliva, urine, and stool, were collected at study enrollment (baseline = the first time point) and longitudinally on average every 3 to 7 days (serial time points). The detailed demographics and clinical characteristics of these 98 subjects are shown in Extended Data Table 1. Plasma and PBMCs were isolated from whole blood, and plasma was used for titer measurements of SARS-CoV-2 spike S1 protein specific IgG and IgM antibodies (anti-S1-IgG and IgM) and cytokine/chemokine measurements. Freshly isolated PBMCs were stained and analysed with flow cytometry[15]. We obtained longitudinal serial time point samples from a subset of these 98 study participants (n = 48, information found in Extended Data Table 1). To compare the immune phenotype between sexes, two sets of data analyses were performed in parallel, baseline and longitudinal as described below. As a control group, COVID-19 uninfected health care workers (HCWs) from Yale-New Haven Hospital were enrolled. Demographics and background information for the HCW group and the demographics of HCWs for cytokine assays and flow cytometry assays for the primary analyses (main figures) are found in Extended Data Table 1. Demographic data, time point information of the samples defined with the days from the symptom onset (DFSO) in each patient, treatment information, and raw data used to generate figures and tables can be found in Supplementary Information Table 1.

Baseline Analysis

The baseline analysis was performed on samples from the first time point of patients who met the following criteria: not in intensive care unit (ICU), had not received tocilizumab (Toci), and had not received high dose corticosteroids (CS; prednisone equivalent >40 mg) before the first sample collection date. This patient group, Cohort A, consisted of 39 patients (17 men and 22 women) (Extended Data Table 1 and 2). The main figures (Fig. 1–4) represent analyses of baseline raw values obtained from patients in Cohort A. In Cohort A patients, male and female patients were matched in terms of age, body mass index (BMI), and DFSO at the first time point sample collection (Extended Data Fig. 1a). However, there were significant differences in age and BMI between HCW controls and patients (patients had higher age and BMI, Extended Data Table 1), therefore an age- and BMI-adjusted difference-in-differences analysis was also performed in parallel (Extended Data Table 3).

Longitudinal Analysis

As parallel secondary analyses, we performed longitudinal analysis on a total patient cohort (Cohort B) to evaluate the difference in immune response over the disease course between male and female patients. Cohort B included all patient samples from Cohort A (including multiple time point samples from the Cohort A patients) as well as an additional 59 patients who did not meet the inclusion criteria for Cohort A. Since Cohort B included more severe patients in ICU, the average clinical scores were higher in Cohort B compared to Cohort A (mean ± SD: 1.3 ± 0.5 (female) and 1.4 ± 0.5 (male) for Cohort A, and 2.5 ± 1.5 (female) and 2.7 ± 1.3 (male) for Cohort B, Extended Data Table 1). This analysis included multiple time point samples from 98 participants in total. Data from Cohort B were analysed for sex differences in immune responses among patients using longitudinal analysis, controlling for potential confounding by age, BMI, receipt of immunomodulatory treatment (Toci and CS), DFSO and ICU status. Second, we conducted a longitudinal analysis comparing male and female COVID-19 patients to male and female HCWs, controlling for age and BMI. Adjusted least square means difference over time in immune response between male and female COVID-19 patients (Extended Data Table 4) and adjusted least square means difference over time in immune response between male and female COVID-19 patients and male and female healthcare workers (Extended Data Table 5) were calculated.

Sex differences in cytokines & chemokines

We first compared the virus RNA concentrations of male and female patients. For both Cohort A and B, there was no difference by sex in terms of viral RNA concentrations in nasopharyngeal swab and saliva. (Fig. 1a, Extended Data Table 3 and 4).

Anti-SARS-CoV-2 S1-specific IgG and IgM (anti-S1-IgG and -IgM) antibodies were comparable in infected men and women in Cohort A (Fig. 1b) and Cohort B (Extended Data Table 4, 5). Thus, at baseline and during disease course, there were no clear differences in the amount of IgG or IgM generated against the S1 protein between male and female patients.

Next, we analysed the levels of 71 cytokines and chemokines in the plasma. Levels of many pro-inflammatory cytokines, chemokines and growth factors, including IL-1β, IL-6, IL-8, TNF, CCL2, CXCL10, and G-CSF, are elevated in the plasma of COVID-19 patients[16]. In line with previous reports, inflammatory cytokine/chemokine levels were generally higher in patients compared with controls (Fig. 1c and Extended Data Fig. 1b and 2a, Extended Data Table 3). Type-I/II/III interferon (IFN) levels were comparable between sexes in Cohort A (Extended Data Fig. 1b, Extended Data Table 3). However, we found higher IFNα2 levels in female patients than male patients in Cohort B (Extended Data Table 4). Levels of many cytokines, chemokines and growth factors were elevated in both men and women compared to HCWs and the levels between sexes were comparable (Fig. 1c and Extended Data Fig. 1b, Extended Data Table 3). However, IL-8 and IL-18 were significantly higher in male patients compared to female patients in Cohort A (Fig. 1c). In age- and BMI-adjusted analysis of Cohort A, we found that although IL-8 and IL-18 were no longer significantly higher among male patients compared directly to female patients, IL-8 and CXCL10 were significantly more elevated in male patients compared to male HCWs than in female patients compared to female HCWs (difference-in-differences, Extended Data Table 3). In adjusted analyses of Cohort B, although we did not see significant sex differences in IL-8 and IL-18, we found significantly higher levels of CCL5 in male patients compared directly to female patients over disease course (Extended Data Table 4) and significantly more elevated CCL5 levels in male patients compared to male HCWs than in female patients compared to female HCWs (Extended Data Table 5, difference-in-differences). These data indicated that, while levels of most of the innate inflammatory cytokines and chemokines were comparable, there were a few factors that are more robustly elevated at the baseline (IL-8 and IL-18) and during disease course (CCL5) in male patients over female patients.

Monocyte differences by sex

Next, we examined the immune cell phenotype by flow cytometry. Freshly isolated PBMCs were stained with specific antibodies to identify T cells, B cells, NK-T cells, NK cells, monocytes, macrophages, and dendritic cells to investigate the PBMC composition (Extended Data Fig. 2b). Consistent with the previous report on T cell decrease in the patients[16], in Cohort A, the proportion of T cells in the live cells was significantly lower in patients, while the proportion of B cells was higher in both male and female patients compared to HCWs (Fig. 2a, Extended Data Table 3). There was no difference in B cell numbers across all groups, but T cell numbers were lower in patients of both sexes (data not shown). In contrast, in Cohort B, we found that male patients had significantly lower T cells, both count and as a proportion of live cells, over disease course compared to female patients

(Extended Data Table 4). Next, we found higher monocyte populations in both sexes in Cohort A (Fig. 2b, c, Extended Data Fig. 2b) compared to HCWs. While $CD14^+CD16^-$ classical monocytes (cMono) were comparable across all groups, levels of $CD14^+CD16^+$ intermediate monocytes (intMono) were elevated in patients compared with HCWs, and this elevation was more robust in female patients (Fig. 2b, c). In contrast, male patients had higher levels of $CD14^{lo}CD16^+$ non-classical monocytes (ncMono) compared to both controls and female patients (Fig. 2b, c). These differences were observed in age- and BMI- adjusted analyses, too, albeit not significant (Extended Data Table 3).

We then divided the 17 Cohort A male patients into two groups, namely, a "high" group who had high percentages of ncMono (upper quartile 4 patients, all had >5% of ncMono) and a "low-int" group (others, 13 patients). We compared age, BMI, DFSO, T cells, and plasma IL-18, and CCL5 levels. While we found no difference in age, BMI, DFSO (Fig. 2d), we noted that high-ncMono group had significantly lower T cell levels and higher plasma CCL5 levels (Fig. 2d). Additionally, we found a significant correlation between CCL5 levels and abundance in ncMono only in male patients (Fig. 2e). These findings suggest that progression from classical to non-classical monocytes may be arrested at the intermediate stage in female patients, and that elevated innate inflammatory cytokines and chemokines are associated with more robust activation of innate immune cells at the baseline as well as more robust longitudinal T cell decrease in male patients.

Higher T cell activation in women

We further examined T cell phenotype in COVID-19 patients. The composition of overall CD4-positive cells and CD8-positive cells among T cells were similar between all groups in Cohort A (Fig. 3a, Extended Data Fig. 2c, Extended Data Table 3). Detailed phenotyping of T cells for naïve T cells, central/effector memory T cells (Tcm/Tem), follicular T cells (Tfh), regulatory T cells (Treg) revealed no remarkable differences in the frequency of these subsets between sexes (Extended Data Fig. 2c). However, we observed higher levels of CD38 and HLA-DR-positive activated T cells in female patients compared to male patients (Fig. 3b, c). In parallel, PD-1 and TIM-3-positive terminally differentiated T cells were more prevalent among female patients compared to male patients (Fig. 3d, e). These findings were seen both in CD4 and CD8 T cells, but the differences were more robust in CD8 T cells (Fig. 3c, e, Extended Data Table 3). We also stained for intracellular cytokines in T cells such as IFNγ, Granzyme B (GzB), TNF, IL-6, and IL-2 for CD8 T cells, and IFNγ, TNF, IL-17A, IL-6, and IL-2 for CD4 T cells. Levels of these cytokines were higher in patients compared to controls, and were generally comparable between sexes in the patients (Extended Data Fig. 2d). Analyses of T cell phenotype in Cohort B did not reveal significant differences between sexes (Extended Data Table 4 and 5). Thus, female COVID-19 patients had more abundant activated and terminally differentiated T cell population than male patients at baseline in unadjusted analyses.

Sex dependent immunity and disease course

We investigated if certain immune phenotypes were correlated with disease trajectory, and whether these phenotypes and factors could be different between sexes. To this end, we evaluated the course of patients in Cohort A. The clinical scores at the first sample collection (C1) were 1 or 2 for all of the Cohort A patients. The patients were categorized into the 'deteriorated' group if the patients marked a score of 3 or higher after the first sample collection date as their maximum clinical scores during admission (Cmax). In contrast, if the patients maintained the score of 1 or 2, they were categorized as 'stabilized' (Extended Data Table 2). Both in male ($N = 17$) and female ($N = 22$) Cohort A patients, 6 patients of each sex deteriorated in their disease course (35.3% and 27.3%, respectively), and the intervals between the dates on which the patients reached Cmax (DFSO at Cmax) and the first sample collection (DFSO at C1) were not significantly different between deteriorated male patients and female patients (mean ± s.d. = 3.7 ± 4.1 and 4.2 ± 2.7, respectively. $P = 0.81$ with unpaired two-tailed t-test).

We first examined age, BMI, viral loads, and anti-S1-IgG antibody titer between the stabilized and deteriorated groups in sex-aggregated manner. We found that the deteriorated group had on average a higher BMI than the stabilized group. While the age was not statistically different, the stabilized group spanned larger age range than the deteriorated, who were in general of more advanced age. The viral load and antibody titers were comparable (Fig. 4a). Next, we examined these factors in a sex-disaggregated manner, and found that the deteriorated male (M_deteriorated) group was on average significantly older compared with stabilized male (M_stabilized) group, while the two female groups (F_deteriorated and F_stabilized) were comparable in age (Fig. 4b). In addition, BMI was higher for M_deteriorated compared to the M_stabilized, while there was no difference between F_deteriorated and F_stabilized groups (Fig. 4b). In contrast, F_deteriorated group had higher saliva viral load than F_stabilized group, while there was no difference in male groups (Fig. 4b). The antibody levels were comparable between deteriorated and stabilized group both in men and women, but stabilized women tended to have higher antibody levels (Fig. 4b).

We further investigated if the key factors identified in the previous analyses correlated with disease progression in male and female patients. We observed that regardless of sex, some chemokines and growth factors, such as CXCL10 (IP-10) and M-CSF, were elevated in patients that went on to develop worse disease. However, there were some innate immune factors, such as CCL5, TNFSF10 (TRAIL) and IL-15, which were specifically elevated only in female patients that subsequently progressed to worse disease, but this difference was not observed in male patients (Fig. 4c). In the age- and DFSO- adjusted analysis of Cohort A, we also found that CCL5 was only elevated in female patients that progressed to worse disease compared to stabilized patients, but no such correlation was found in men (Extended Data Table 6).

T cell phenotypes in these groups revealed that male patients whose disease worsened had a significantly lower proportion of activated T cell ($CD38^+HLA\text{-}DR^+$) and terminally differentiated T cell ($PD\text{-}1^+TIM\text{-}3^+$) and tendencies for fewer IFNγ+ CD8 T cells at the first sample collection, compared with their counterpart men who progressed to worse disease (Fig. 4d). However, in women, the deteriorated group had similar levels of these types of CD8 T cells compared with the stabilized group (Fig. 4d).

We finally examined the correlations between age, BMI, viral loads, anti-S1 antibodies, cytokines/chemokines, activated/terminally differentiated/IFNγ-producing CD8 T cells, and clinical disease course (Cmax − C1 was used for the deterioration score). The correlation matrix clearly revealed that in women higher innate immune cytokines, such as TNFSF10 and IL-15, were positively correlated with disease progression, while there was no association between CD8 T cell status and deterioration (Fig. 4e, results of age- and DFSO- adjusted analysis in Extended Data Table 6). In particular, CXCL10, M-CSF, and IL-15 were positively correlated with $IFN\gamma^+CD8$ T cells in female patients (Fig. 4d).

In contrast, in male patients, progressive disease was clearly associated with higher age, higher BMI, and poor CD8 T cell activation (Fig. 4e). Poor CD8 T cell activation and poor IFNγ production by CD8 T cells were significantly correlated with patients' age, while these correlations were not seen in female patients (Fig. 4e, f). These differences seemed to highlight the differences between the sexes in the immune response against SARS-CoV-2 as well as the difference of the potential prognostic/predictive factors for clinical deterioration of COVID-19.

Discussion

Our results revealed key differences in immune responses during the disease course of SARS-CoV-2 infection in male and female patients. First, we found that the levels of several important proinflammatory innate immune chemokines and cytokines such as IL-8, IL-18 (at baseline), and CCL5 (longitudinal analysis) were higher in male patients, which correlated with higher non-classical monocytes (at baseline). Second, we observed a more robust T cell response among female patients compared to male patients at baseline. In particular, activated CD8 T cells were significantly elevated only in female patients but not in male patients over healthy volunteers. Analysis of their clinical trajectory revealed that, while poor T cell responses were associated with future progression of disease in male patients, higher innate immune cytokine levels were associated with worsening of COVID-19 disease in female patients. Importantly, the T cell response was significantly and negatively correlated with patients' age in male, but not female, patients. These data indicate key differences in the baseline immune capabilities in men and women during the early phase of SARS-COV-2 infection, and suggest a potential immunological underpinning of the distinct mechanisms of disease progression between sexes. These analyses also provide a potential basis for taking sex-dependent approaches to prognosis, prevention, care, and therapy for patient with COVID-19.

While we believe our study provides a strong basis for further investigation into how COVID-19 disease dynamics may differ between men and women, it is important to note that there are some limitations to the analyses presented in this manuscript. First, we acknowledge that the healthy HCWs used as the control population were not matched to patients based on age, BMI or underlying risk factors. To account for this, we performed adjusted analyses for the baseline and longitudinal comparisons between patients (Cohort A and the full patient population, Cohort B) and HCWs, controlling for age and BMI. However, we cannot rule out residual confounding due to underlying risk factors not available for the HCW controls.

Collectively, these data suggest that vaccines and therapies to elevate T cell immune response to SARS-CoV-2 might be warranted for male patients, while female patients might benefit from therapies that dampen innate immune activation early during disease. Immune landscape in COVID-19 patients is considerably different between the sexes, and these differences may underlie heightened disease susceptibility in men.

Online content

Any methods, additional references, Nature Research reporting summaries, source data, extended data, supplementary information, acknowledgements, peer review information; details of author contributions and competing interests; and statements of data and code availability are available at https://doi.org/10.1038/s41586-020-2700-3.

1. Chen, N. et al. Epidemiological and clinical characteristics of 99 cases of 2019 novel coronavirus pneumonia in Wuhan, China: a descriptive study. *Lancet* **395**, 507–513 (2020). https://doi.org/10.1016/S0140-6736(20)30211-7.
2. Li, Q. et al. Early Transmission Dynamics in Wuhan, China, of Novel Coronavirus-Infected Pneumonia. *N. Engl. J. Med.* **382**, 1199–1207 (2020). https://doi.org/10.1056/NEJMoa2001316.
3. Yang, X. et al. Clinical course and outcomes of critically ill patients with SARS-CoV-2 pneumonia in Wuhan, China: a single-centered, retrospective, observational study. Lancet *Respir. Med.* **8**, 475–481 (2020). https://doi.org/10.1016/S2213-2600(20)30079-5.
4. Meng, Y. et al. Sex-specific clinical characteristics and prognosis of coronavirus disease-19 infection in Wuhan, China: A retrospective study of 168 severe patients. *PLoS Pathog.* **16**, e1008520 (2020). https://doi.org/10.1371/journal.ppat.1008520.
5. Gebhard, C., Regitz-Zagrosek, V., Neuhauser, H. K., Morgan, R. & Klein, S. L. Impact of sex and gender on COVID-19 outcomes in Europe. *Biol. Sex Differ.* **11**, 29 (2020). https://doi.org/10.1186/s13293-020-00304-9.
6. Zhu, N. et al. A Novel Coronavirus from Patients with Pneumonia in China, 2019. *N. Engl. J. Med.* **382**, 727–733 (2020). https://doi.org/10.1056/NEJMoa2001017.
7. World Health Organization (WHO) Director-General's opening remarks at the media briefing on COVID-19 - 11 March 2020, https://www.who.int/dg/speeches/detail/who-director-general-s-opening-remarks-at-the-media-briefing-on-covid-19—11-march-2020.
8. Williamson, E. J. et al. Factors associated with COVID-19-related death using OpenSAFELY. *Nature* (2020). https://doi.org/10.1038/s41586-020-2521-4 .
9. Klein, S. L. & Flanagan, K. L. Sex differences in immune responses. *Nat. Rev. Immunol.* **16**, 626–638 (2016). https://doi.org/10.1038/nri.2016.90.
10. Fischer, J., Jung, N., Robinson, N. & Lehmann, C. Sex differences in immune responses to infectious diseases. *Infection* **43**, 399–403 (2015). https://doi.org/10.1007/s15010-015-0791-9.
11. Guerra-Silveira, F. & Abad-Franch, F. Sex bias in infectious disease epidemiology: patterns and processes. *PLoS One* **8**, e62390 (2013). https://doi.org/10.1371/journal.pone.0062390.
12. Moore, A. L. et al. Virologic, immunologic, and clinical response to highly active antiretroviral therapy: the gender issue revisited. *J. Acquir. Immune Defic. Syndr.* **32**, 452–461 (2003). https://doi.org/10.1097/00126334-200304010-00017.
13. Collazos, J., Asensi, V. & Cartón, J. A. Sex differences in the clinical, immunological and virological parameters of HIV-infected patients treated with HAART. *AIDS* **21**, 835–843 (2007). https://doi.org/10.1097/QAD.0b013e3280b0774a.
14. Fink, A. L., Engle, K., Ursin, R. L., Tang, W. Y. & Klein, S. L. Biological sex affects vaccine efficacy and protection against influenza in mice. *Proc. Natl Acad. Sci. USA* **115**, 12477–12482 (2018). https://doi.org/10.1073/pnas.1805268115.
15. Lucas, C. et al. Longitudinal analyses reveal immunological misfiring in severe COVID-19. *Nature* (2020). https://doi.org/10.1038/s41586-020-2588-y.
16. Huang, C. et al. Clinical features of patients infected with 2019 novel coronavirus in Wuhan, China. *Lancet* **395**, 497–506 (2020). https://doi.org/10.1016/S0140-6736(20)30183-5.

Yale IMPACT research team

Kelly Anastasio[14], Michael H. Askenase[15], Maria Batsu[16], Hannah Beatty[16], Santos Bermejo[16], Sean Bickerton[17], Kristina Brower[2], Molly L. Bucklin[1], Staci Cahill[14], Melissa Campbell[3], Yiyun Cao[1], Edward Courchaine[17], Rupak Datta[3], Giuseppe DeLuliis[8], Bertie Geng[16], Laura Glick[16], Ryan Handoko[16], Chaney Kalinich[2], William Khoury-Hanold[1], Daniel Kim[1], Lynda Knaggs[16], Maxine Kuang[14], Eriko Kudo[1], Joseph Lim[18], Melissa Linehan[1], Alice Lu-Culligan[1], Amyn A. Malik[11], Anjelica Martin[1], Irene Matos[16], David McDonald[16], Maksym Minasyan[16], Subhasis Mohanty[3], M. Catherine Muenker[2], Nida Naushad[16], Allison Nelson[16], Jessica Nouws[16], Marcella Nunez-Smith[19], Abeer Obaid[16], Isabel Ott[2], Hong-Jai Park[16], Xiaohua Peng[16], Mary Petrone[2], Sarah Prophet[20], Harold Rahming[16], Tyler Rice[1], Kadi-Ann Rose[16], Lorenzo Sewanan[16], Lokesh Sharma[8], Denise Shepard[16], Erin Silva[16], Michael Simonov[16], Mikhail Smolgovsky[16], Eric Song[1], Nicole Sonnert[1], Yvette Strong[16], Codruta Todeasa[16], Jordan Valdez[16], Sofia Velazquez[15], Pavithra Vijayakumar[16], Haowei Wang[3], Annie Watkins[2], Elizabeth B. White[2] & Yexin Yang[1]

[14]Yale Center for Clinical Investigation, Yale University School of Medicine, New Haven, CT, 06520, USA. [15]Department of Neurology, Yale University School of Medicine, New Haven, CT, 06520, USA. [16]Yale School of Medicine, New Haven, CT, 06520, USA. [17]Department of Biochemistry and of Molecular Biology, Yale University School of Medicine, New Haven, CT, 06520, USA. [18]Yale Viral Hepatitis Program, Yale University School of Medicine, New Haven, CT, 06520, USA. [19]Equity Research and Innovation Center, Yale University, New Haven, CT, 06520, USA. [20]Department of Molecular, Cellular and Developmental Biology, Yale University School of Medicine, New Haven, CT, 06520, USA.

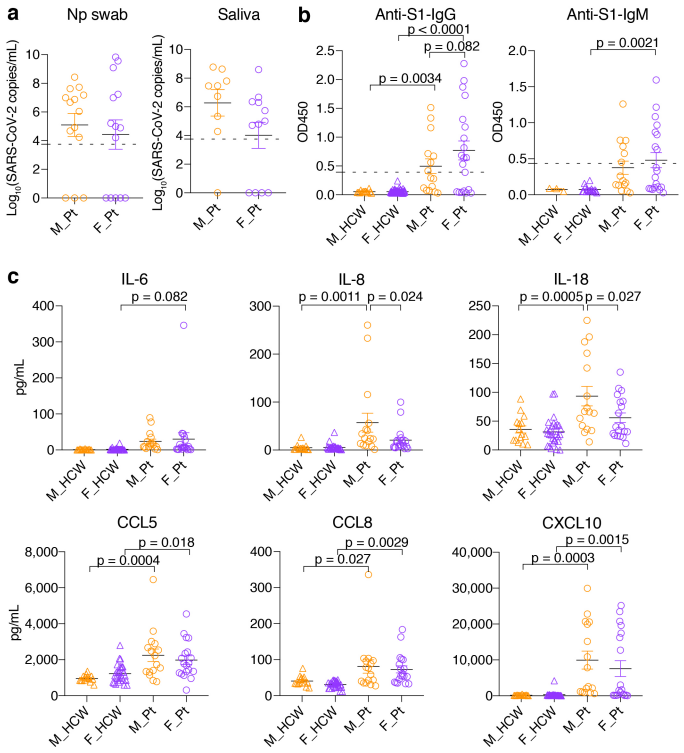

Fig. 1 | Comparison of virus RNA concentrations, anti-SARS-CoV-2 antibody titers, and plasma cytokines and chemokine levels at the first sampling of Cohort A patients. a, Comparison of virus RNA measured from nasopharyngeal (Np) swab and saliva. Both $n = 14$ for male (M_Pt) and Female patients (F_Pt) for nasopharyngeal samples, and $n = 9$ and 12, respectively, for saliva samples. Dotted lines indicate the detection limit of the assay (5,610 copies/mL), and negatively tested data are shown on the *x*-axis (not detected; ND). **b**, Titers of specific IgG and IgM antibody titers against SARS-CoV-2 S1 protein were measured. $n = 13, 74, 15$, and 20 for IgG, and $n = 3, 18, 15$, and 20 for IgM, for male HCW (M_HCW), female HCW (F_HCW), M_Pt, and F_Pt, respectively. The cutoff values for the positivity are shown with the dotted lines. **c**, Comparison of the plasma levels of representative innate immune cytokines and chemokines. $n = 15, 28, 16$, and 19 for M_HCW, F_HCW, M_Pt, and F_Pt, respectively. Unpaired two-tailed *t*-test was used in **a** and one-way ANOVA with Bonferroni multiple comparison test was used in **b** and **c**. All p-values <0.10 are shown. Data are mean ± SEM. The results of all the cytokines/chemokines measured including those shown here can be found in Extended Data Fig. 1b.

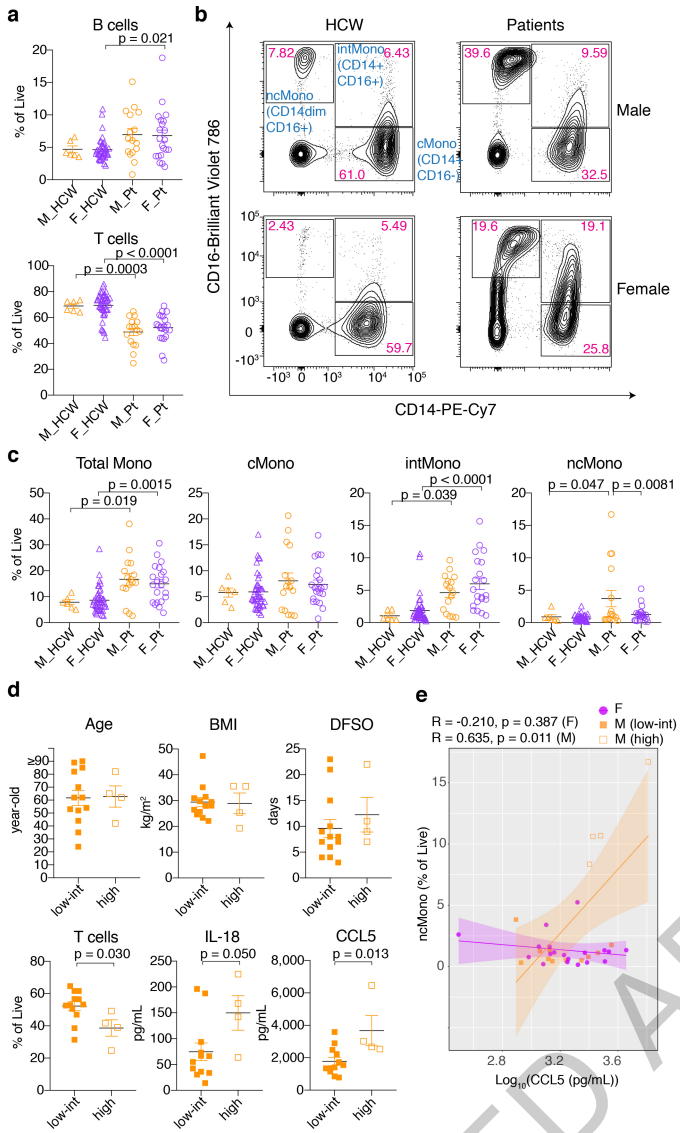

Fig. 2 | PBMC composition differences between male and female Cohort A patients at the first sampling. a, Comparison on the proportion of B cells and T cells in live PBMCs. *n* = 6, 42, 16, and 21 for M_HCW, F_HCW, M_Pt, and F_Pt, respectively. **b**, Representative 2D plots for CD14 and CD16 in monocytes gate (live/singlets/CD19-CD3-/CD56-CD66b-). Numbers in red indicate the percentages of each population in the parent monocyte gate. **c**, Comparison between percentages of total Monocytes, cMono, intMono, ncMono in the live PBMCs. *n* = 6, 42, 16, and 21 for M_HCW, F_HCW, M_Pt, and F_Pt, respectively. **d**, Comparison of age, BMI, DFSO, T cells (% of live PBMCs), and plasma IL-18/CCL5 levels between male patients who had high ncMono and low-intermediate ncMono. *n* = 13 and 4 for "low-int" group and "high" group, respectively, for age, BMI and DFSO. *n* = 12 and 4 for "low-int" group and "high" group, respectively, for T cells and IL-18/CCL5 levels. **e**, Correlation between plasma CCL5 levels and ncMono (% of live cells). Pearson correlation coefficients (R) and p-values for each sex are shown on top of the plot. ncMono-high male patients (*n* = 4) are shown with orange open squares, and ncMono-low-int male patients (*n* = 11) are shown with orange closed squares. *n* = 19 for female patients (purple circles). Data are mean ± SEM in **a**, **c**, and **d**. One-way ANOVA with Bonferroni multiple comparison test was used in **a** and **c**, and unpaired two-tailed *t*-test used in **d**. All p-values <0.10 are shown in the panels.

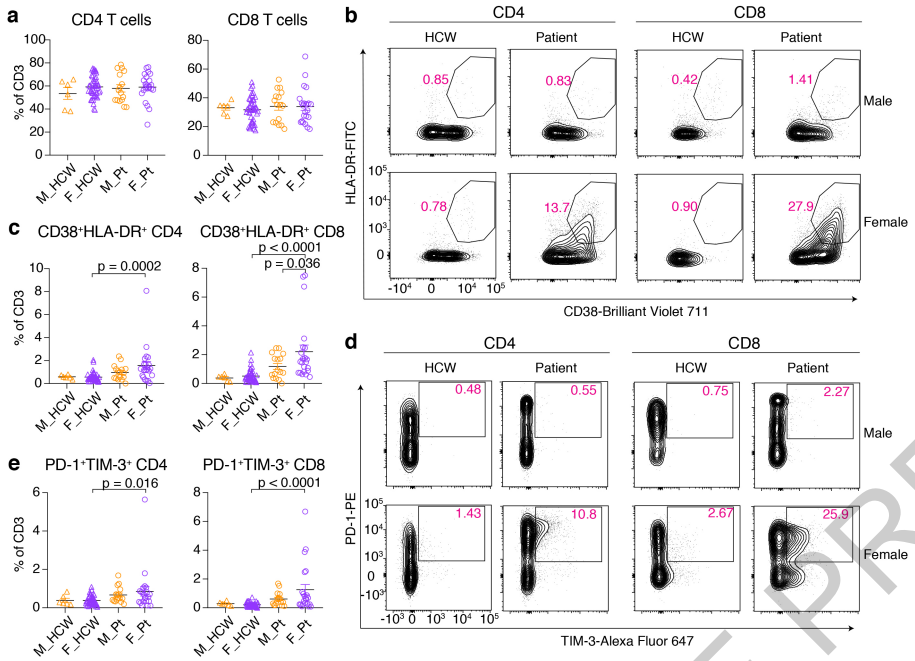

Fig. 3 | Sex difference in T cell phenotype at the first sampling of Cohort A patients. a, Percentages of CD4 and CD8 in the CD3-positive cells. **b**, Representative 2D plots for CD38 and HLA-DR in the CD4 and CD8 T cells. Numbers in red indicate the percentages of $CD38^+HLA\text{-}DR^+$ populations in the parent gate (live/singlets/$CD3^+$/$CD4^+$ or $CD8^+$). **c**, Percentages of $CD38^+HLA\text{-}DR^+$ CD4/CD8 cells in CD3-positive cells are summarized. **d**, Representative 2D plots for PD-1 and TIM-3 in the CD4 and CD8 T cells are shown. Numbers in red indicate the percentages of $PD\text{-}1^+TIM\text{-}3^+$ populations in the parent gate (live/singlets/$CD3^+$/$CD4^+$ or $CD8^+$/$CD45RA^-$). **e**, Percentages of $PD\text{-}1^+TIM\text{-}3^+$ CD4/8 cells in CD3-positive cells are summarized. $n = 6, 45, 16$, and 22 for M_HCW, F_HCW, M_Pt, and F_Pt, respectively, and one-way ANOVA with Bonferroni multiple comparison test was used for the comparisons in **a, c**, and **e**. Data are mean ± SEM. All p-values <0.10 are shown in the panels.

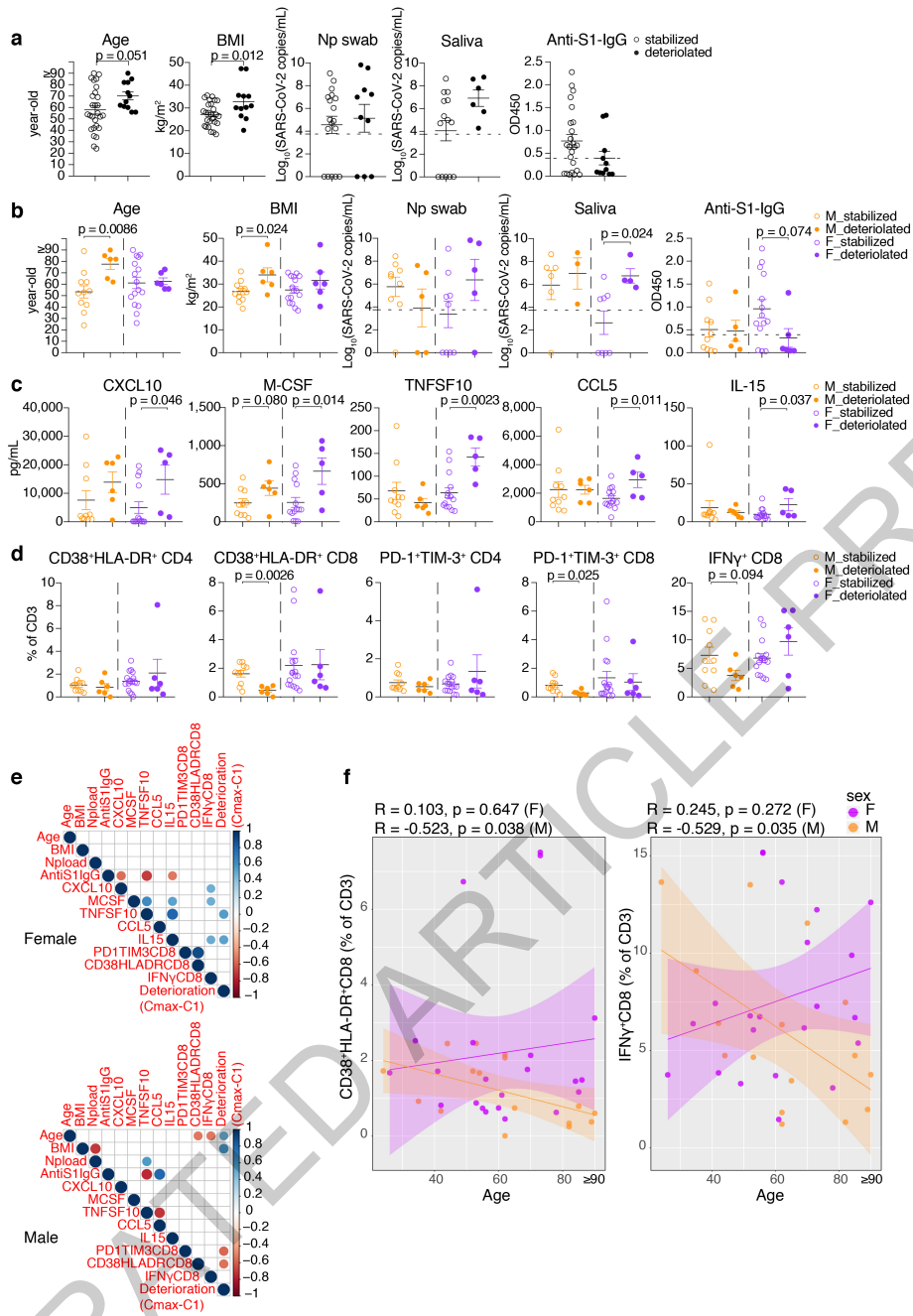

Fig. 4 | Differential immune phenotypes at the first sampling and disease progression between sexes in Cohort A patients. Sex-aggregated (**a**) and disaggregated (**b**) comparison of age, BMI, RNA concentration in nasopharyngeal swab and Saliva, and anti-S1-IgG between stabilized and deteriorated group. $n = 11, 6, 16$, and 6 for age and BMI, $n = 9, 5, 9$, and 5 for nasopharyngeal swab, $n = 6, 3, 8$, and 4 for saliva, and $n = 10, 5, 14$, and 6 for anti-S1-IgG, for M_stabilized, M_deteriorated, F_stabilized, and F_deteriorated group, respectively. Dotted lines in virus concentration panels and anti-S1-IgG panels indicate the detection limit and cutoff value for positivity, respectively. **c**, Cytokine/chemokine comparison between stabilized and deteriorated groups. $n = 10, 6, 14$, and 5 for M_stabilized, M_deteriorated, F_stabilized, and F_deteriorated group, respectively. **d**, Comparisons in the proportions of activated ($CD38^+HLA\text{-}DR^+$) and terminally differentiated ($PD\text{-}1^+TIM\text{-}3^+$) CD4/CD8 T cells, and $IFN\gamma^+$CD8 T cells in CD3-positive T cells are shown. $n = 10, 6, 16$, and 6 for M_stabilized, M_deteriorated, F_stabilized, and F_deteriorated group, respectively. **e**, Pearson correlation heatmaps of the indicated parameters are shown for each sex. For viral RNA concentrations and cytokine/chemokine levels, log-transformed values were used for the calculation of the correlations. The size and colour of the circles indicate the correlation coefficient (R), and only statistically significant correlations ($P < 0.05$) are shown. Clinical deterioration from the first time point was scored by Cmax-C1. $n = 17$ and 22 for male and female, respectively. **f**, Correlation between age and $CD38^+HLA\text{-}DR^+$ CD8 T cells (left) and $IFN\gamma^+$CD8 T cells (right). Pearson correlation coefficient (R) and p-values for each correlation and for each sex are shown on top of each plot. Unpaired two-tailed *t*-test was used to compare the differences between stabilized group and deteriorated group in **a**, **b**, **c**, and **d**. Data are mean ± SEM. All p-values <0.10 are shown in the panels.

Methods

Ethics statement

This study was approved by Yale Human Research Protection Program Institutional Review Boards (FWA00002571, Protocol ID. 2000027690). Informed consents was obtained from all enrolled patients and healthcare workers.

Patients and HCWs

Adult patients (≥18 years old) admitted to Yale-New Haven Hospital between March 18th and May 9th, 2020, positive for SARS-CoV-2 by RT–PCR from nasopharyngeal and/or oropharyngeal swabs, and able to provide informed consent (surrogate consent accepted) were eligible for the Yale IMPACT Biorepository study, and 198 patients were enrolled in this period. All patients necessitated hospitalization for their symptoms and had WHO score (Ref. [17]) ≥ 3 at admission (= Hospitalized Mild disease). At the initial screening, clinical PCR tests were performed in CLIA-certified laboratory and only the PCR-positive patients were enrolled. Only after the confirmation of PCR-positivity, the patients were enrolled and the first time point samples for this study were collected for each patient. The first time point samples were collected at 11.4 ± 8.1, 10.2 ± 6.3, 11.7 ± 7.2, and 12.1 ± 7.3 (mean ± SD) days after the symptom onset (DFSO) in Cohort A female, Cohort A male, Cohort B female, and Cohort B male, respectively (Extended Data Fig. 1a right panel for Cohort A and Extended Data Table 1).

Among these patients, we could obtain whole blood for flow cytometry analysis using fresh PBMCs, plasma for cytokine/chemokine measurements, anti-S1 antibody measurements and nasopharyngeal swab and saliva from total of 98 individuals for the present study. For longitudinal analyses, biospecimens (blood, nasopharyngeal swabs, saliva, urine, and/or stool) were collected at study enrollment (baseline) and on average every 3 to 7 days while in the hospital in 48 of these 98 patients.

The patients were assessed with a locally developed clinical scoring system for disease severity; 1: admitted and observed without supplementary oxygen, 2: required ≤ 3L supplementary oxygen via nasal canal to maintain SpO2 > 92%, 3: received tocilizumab, which per hospital treatment protocol required that the patient to require >3L supplementary oxygen to maintain SpO2 > 92%, or, required >2L supplementary oxygen to maintain SpO2 > 92% and had a high sensitivity C-reactive protein (CRP) > 70. 4: the patient required intensive care unit (ICU) level care, 5: the patient required intubation and mechanical ventilation. In relation to the WHO scoring[17], our clinical score 1, 2/3, 4, 5 largely correspond to WHO score 3, 4, 5, 6/7, respectively. Detailed demographic information for the entire cohort (98 Cohort B patients, and multiple time point samples from 54 patients among them) and of Cohort A (39 patients) are shown in Extended Data Table 1-3. For the patients who are 90-year-old or older, their ages were protected health information, and 90 was put as the surrogate value for the analyses. Among total 198 patients enrolled in IMPACT study in this period, we obtained whole blood, nasopharyngeal swabs or saliva samples from in total 98 patients for the present study. Individuals with active chemotherapy against cancers, pregnant patients, patients with background hematological abnormalities, patients with autoimmune diseases and patients with a history of organ transplantation and on immunosuppressive agents, were excluded from this study.

As a control group, COVID-19 uninfected HCWs from Yale-New Haven Hospital were enrolled. HCWs were tested every 2 weeks for PCR and serology. For the control group, the PBMCs and plasma analysis were done when both tests were negative. In other words, if either or both of these tests were positive, these samples were excluded from the analyses. In some HCWs, samples up to two time points were collected for the assays. In these cases, if the data for a certain type of assay were available for both of these time points, only the first time point data were used and otherwise data for either time point were used in the main analyses with Cohort A.

Virus RNA measurement

SARS-CoV-2 RNA concentrations were measured from nasopharyngeal samples and saliva samples by RT–PCR as previously described[18,19]. In short, total nucleic acid was extracted from 300 µl of viral transport media from the nasopharyngeal swab or 300 µl of whole saliva using the MagMAX Viral/Pathogen Nucleic Acid Isolation kit (ThermoFisher Scientific) using a modified protocol and eluted into 75 µl of elution buffer[19]. For SARS-CoV-2 RNA detection, 5 µl of RNA template was tested as previously described[18], using the US CDC real-time RT–PCR primer/probe sets for 2019-nCoV_N1, 2019-nCoV_N2, and the human RNase P (RP) as an extraction control. Virus RNA copies were quantified using a tenfold dilution standard curve of RNA transcripts that we previously generated[18]. If the RNA concentration was lower than the limit of detection (ND) which was determined previously[18], the value was set to 0 and used for the analyses.

Isolation of plasma

Plasma samples were collected after whole blood centrifugation at 400 g for 10 min at RT with brake off. The plasma was then carefully transferred to 15 ml conical tubes and then aliquoted and stored at -80 °C for subsequent analysis.

SARS-CoV-2 specific antibody titer measurement

ELISAs were performed as previously described[20]. In short, Triton X-100 and RNase A were added to serum samples at final concentrations of 0.5% and 0.5 mg/ml respectively and incubated at room temperature (RT) for 30 min before use to reduce risk from any potential virus in serum. 96-well MaxiSorp plates (Thermo Scientific #442404) were coated with 50 µl/well of recombinant SARS-CoV-2 S1 protein (ACROBiosystems #S1N-C52H3-100 µg) at a concentration of 2 µg/ml in PBS and were incubated overnight at 4 °C. The coating buffer was removed, and plates were incubated for 1 h at RT with 200 µl of blocking solution (PBS with 0.1% Tween-20, 3% milk powder). Serum was diluted 1:50 in dilution solution (PBS with 0.1% Tween-20, 1% milk powder) and 100 µl of diluted serum was added for two hours at RT. Plates were washed three times with PBS-T (PBS with 0.1% Tween-20) and 50 µl of HRP anti-Human IgG Antibody (GenScript #A00166, 1:5000) or anti-Human IgM-Peroxidase Antibody (Sigma-Aldrich #A6907, 1:5000) diluted in dilution solution were added to each well. After 1 h of incubation at RT, plates were washed six times with PBS-T. Plates were developed with 100 µl of TMB Substrate Reagent Set (BD Biosciences #555214) and the reaction was stopped after 12 min by the addition of 100ul of 2 N sulfuric acid. Plates were then read at a wavelength of 450 nm and 570nm.

The cutoff values for sero-positivity were determined as 0.392 and 0.436 for anti-S1-IgG and anti-S1 IgM, respectively. Eighty pre-pandemic plasma samples were assayed to establish the negative baselines, and these values were statistically determined with confidence level of 99%.

Cytokine and chemokine measurement

Patients' sera isolated as above were stored in -80 °C until the measurement of the cytokines. The sera were shipped to Eve technologies (Calgary, Alberta, Canada) on dry ice, and levels of 71 cytokines and chemokines were measured with Human Cytokine Array/Chemokine Array 71-Plex Panel (HD71). All the samples were measured upon the first thaw.

The shipment of the samples and measurements were done in two separate batches, but the measurements were performed with the same assay kits using the same standard curves, therefore minimizing the batch effects between the measurements.

For the out of range values of the measurements, either the lowest/highest extrapolatable values or the lowest/highest standard curve

were recorded following the instructions of HD71 assay, and included in the analyses. Among all the samples measured, we found that two samples had outlier values (beyond 1.5x interquartile range) in more than half of the 71 cytokines/chemokines measured, suggesting the technical error and/or poor sample qualities in the measurements. Therefore, cytokine/chemokine data of these individuals were excluded from the analyses.

Isolation of PBMCs

The peripheral blood mononuclear cells (PBMCs) were isolated from heparinized whole blood using Histopaque density gradient under the biosafety level 2+ facility. To isolate PBMCs, blood 1:1 diluted in PBS was layered over in Histopaque in a SepMate tube and centrifuged for 10 min at 1200g. The PBMC layer was collected by quickly pouring the content into a new 50ml tube. The cells were washed twice with PBS to remove any remaining histopaque and to remove platelets. The pelleted cells were treated with ACK buffer for red cell lysis and then counted. The percentage viability was estimated using Trypan blue staining.

Flow cytometry

Using the freshly isolated PBMCs, the staining was performed in three separate panels for 1) PBMC cell composition, 2) T cell surface staining, and 3) T cell intracellular staining. Exact antibody clones and vendors that were used for flow cytometric analysis are as follows: BB515 anti-HLA-DR (G46-6), BV785 anti-CD16 (3G8), PE-Cy7 anti-CD14 (HCD14), BV605 anti-CD3 (UCHT1), BV711 anti-CD19 (SJ25C1), BV421 anti-CD11c (3.9), AlexaFluor647 anti-CD1c (L161), Biotin anti-CD141 (M80), PE anti-CD304 (12C2), APCFire750 anti-CD11b (ICRF44), PerCP/Cy5.5 anti-CD66b (G10F5), BV785 anti-CD4 (SK3), APCFire750 or PE-Cy7 or BV711 anti-CD8 (SK1), BV421 anti-CCR7 (G043H7), AlexaFluor 700 anti-CD45RA (HI100), PE anti-PD1 (EH12.2H7), APC anti-TIM3 (F38-2E2), BV711 anti-CD38 (HIT2), BB700 anti-CXCR5 (RF8B2), PE-Cy7 anti-CD127 (HIL-7R-M21), PE-CF594 anti-CD25 (BC96), BV711 anti-CD127 (HIL-7R-M21), BV421 anti-IL17a (N49-653), AlexaFluor 700 anti-TNFa (MAb11), PE or APC/Fire750 anti-IFNy (4S.B3), FITC anti-GranzymeB (GB11), AlexaFluor 647 anti-IL4 (8D4-8), BB700 anti-CD183/CXCR3 (1C6/CXCR3), PE-Cy7 anti-IL-6 (MQ2-13A5), PE anti-IL-2 (5344.111), BV785 anti-CD19 (SJ25C1), BV421 anti-CD138 (MI15), AlexaFluor700 anti-CD20 (2H7), AlexaFluor 647 anti-CD27 (M-T271), PE/Dazzle594 anti-IgD (IA6-2), PE-Cy7 anti-CD86 (IT2.2), APC/Fire750 anti-IgM (MHM-88), BV605 anti-CD24 (M1/69), APC/Fire 750 anti-CD10 (HI10a), BV421 anti-CD15 (SSEA-1), AlexaFluor 700 Streptavidin (ThermoFisher). Freshly isolated PBMC were plated at 1-2x10^6 cells in a 96 well U-bottom plate. Cells were resuspended in Live/Dead Fixable Aqua (ThermoFisher) for 20 min at 4 °C. Following a wash, cells were then blocked with Human TruStan FcX (BioLegend) for 10 min at RT. Cocktails of desired staining antibodies were directly added to this mixture for 30 min at RT. For secondary stains, cells were washed and supernatant aspirated; to each cell pellet, a cocktail of secondary markers was added for 30 min at 4 °C. Prior to analysis, cells were washed and resuspended in 100 µL of 4% PFA for 30 min at 4 °C. For intracellular cytokine staining following stimulation, cells were resuspended in 200 µL cRPMI (RPMI-1640 supplemented with 10% FBS, 2 mM L-glutamine, 100 U/ml penicillin, and 100 mg/ml streptomycin, 1 mM Sodium Pyruvate, and 50 µM 2-Mercaptoethanol) and stored at 4 °C overnight. Subsequently, these cells were washed and stimulated with 1X Cell Stimulation Cocktail (eBioscience) in 200 µL cRPMI for 1 h at 37 °C. Directly to this, 50 µL of 5X Stimulation Cocktail (plus protein transport inhibitor) (eBioscience) was added for an additional 4 h of incubation at 37 °C. Following stimulation, cells were washed and resuspended in 100 µL of 4% PFA for 30 min at 4 °C. To quantify intracellular cytokines, these samples were permeabilized with 1X Permeabilization Buffer from the FOXP3/ Transcription Factor Staining Buffer Set (eBioscience) for 10 min at 4 °C. All further staining cocktails were made in this buffer. Permeabilized cells were then washed and resuspended in a cocktail containing Human TruStan FcX (BioLegend) for 10 min at 4 °C. Finally, intracellular staining cocktails were directly added to each sample for 1 h at 4 °C. Following this incubation, cells were washed and prepared for analysis on an Attune NXT (ThermoFisher). Data were analysed using FlowJo software version 10.6 software (Tree Star).

Set of markers used to identify each subset of cells are summarized in Extended Data Table 7, and gating strategies for the key cell populations presented in the main figures are shown in Extended Data Fig. 3a-c. For the majority of samples, all available staining panels were implemented and analysed. The few exceptions pertained to those samples during which a mechanical malfunction occurred, which depleted the sample before acquisition, or to the samples with poor staining qualities. In these cases, data for these samples or panels were missing and not available. All the data available were used for the analyses, and the data used to generate figures and tables can be found in Supplementary Information Table 1, and the raw fcs files are available at ImmPort as described in Data Availability.

Statistical analysis for the primary analyses

For the primary analyses shown in the main figures, Graph Pad Prism (v8.0) was used for all statistical analysis. Unless otherwise noted, one-way ANOVA with Bonferroni's multiple comparison test was used for the comparisons between M_Pt vs F_Pt, M_Pt vs M_HCW, F_Pt vs F_HCW, and M_HCW vs F_HCW for the comparisons. For two-group comparisons including the comparison between stabilized group and deteriorated group in each sex (Fig. 4 a–d), two-sided unpaired *t*-test was used for the comparison. Bioconductor R (version 3.6.3) package ggplot2 (version 3.3.0) was used to generate heatmaps (Extended Data Fig. 2), XY graphs for correlation analyses (Fig. 2e, 4f), and Pearson correlation heatmaps (Fig. 4e).

Statistical analysis for the secondary analyses

All multivariable analyses were conducted using R version 3.6.1 (for data cleaning) and SAS version 9.4 (Cary, NC; for data analysis). The code used for data cleaning and data analysis is available at https://github.com/muhellingson/covid_immresp. We conducted longitudinal analyses of the differences in immune response by sex for patients with COVID-19 and differences in immune response between patients with COVID-19 and healthcare workers by sex and adjusted linear regression to evaluate differences in immune response by sex at baseline and the differences in immune response by sex and patient trajectory.

Longitudinal difference in immune response in all COVID-19 positive patients (Cohort B) by sex. A marginal linear model was fit to evaluate the difference in various immune responses (outcome) in patients by sex (exposure). We used an auto-regressive correlation structure to account for correlation between repeated observations in an individual over time. To account for the small sample size and unequal follow-up between participants, we used the Morel-Bokossa-Neerchal (MBN) correction. In addition to sex, the model contained time-independent terms for age (in years) and BMI and time-dependent terms for days from symptom onset (self-reported), ICU status (as a proxy for disease severity) and treatment with either tocilizumab or corticosteroids. A patient was defined as 'on tocilizumab' at a given time point if they had received the treatment within fourteen days before the time the sample was taken. Patients were defined as 'on corticosteroids' if they had received the treatment on the same day the sample was taken. The resulting regression coefficients were interpreted as the difference in the adjusted least square means immune response between female and male patients.

Difference in immune response between COVID-19 positive patients (Cohort A) and healthcare workers by sex at baseline. We used linear regression to evaluate the difference in immune response between female and male patients at the first time point for those patients who

had not received corticosteroids or toci before enrollment (Cohort A). The model contained terms for sex, patient trajectory (worsened vs. stable), age, BMI, and an interaction term for sex and group (patient versus healthcare worker). We calculated the least square means for each group (female patients who worsened, female patients who stabilized, male patients who worsened and male patients who stabilized) and evaluated the differences in the least square means of the different immune response outcomes by group and sex. P-values and 95% confidence intervals were calculated with a Tukey correction for multiple pairwise comparisons. The regression coefficient of the interaction term between sex and group was interpreted as the difference-in-differences of the two comparison by sex or by group (for example, the difference-in-differences between female and male patients and female and male healthcare workers).

Longitudinal difference in immune response between all COVID-19 positive patients (Cohort B) and healthcare workers by sex. We used a marginal linear model with a compound symmetric correlation structure and the MBN correction to evaluate the difference in immune responses between patients and healthcare workers by sex, controlling for age and BMI. We calculated the least square means for each group (female patients, female healthcare workers, male patient, male healthcare workers) and evaluated the differences in adjusted least square means to compare study groups by sex (female patients vs. male patients, female healthcare workers vs. male healthcare workers, female patients vs. female healthcare workers and male patients vs. male healthcare workers). P-values and 95% Confidence intervals were corrected using the Tukey correction for multiple pairwise comparisons. The regression coefficient of the interaction term between sex and study group was interpreted as the difference-in-differences between the two comparisons by sex or by group.

Multivariable patient trajectory analysis. We used linear regression to evaluate the difference in baseline immune response between patients who worsened after the baseline sample was taken and those who stabilized by sex. The model contained terms for sex, patient trajectory (worsened vs. stable), age, days from symptom onset and an interaction term for sex and patient trajectory. We calculated the adjusted least square means for each group (female patients who worsened, female patients who stabilized, male patients who worsened and male patients who stabilized) and evaluated the differences in least square means of the different immune responses by patient trajectory and sex using the Tukey correction for multiple comparisons. The regression coefficient of the interaction term between sex and patient trajectory was interpreted as the difference-in-differences between the two patient trajectories by sex or sex by the two patient trajectories.

Reporting summary

Further information on research design is available in the Nature Research Reporting Summary linked to this paper.

Data availability

All of the background information of HCWs, clinical information of patients, and raw data used in this study are included in the Supplementary Information Table 1. Additionally, all of the raw fcs files for the flow cytometry analysis are uploaded in ImmPort (https://www.immport.org/shared/home, Study ID: SDY1648).

17. WHO R&D Blueprint novel Coronavirus COVID-19 Therapeutic Trial Synopsis. https://www.who.int/blueprint/priority-diseases/key-action/COVID-19_Treatment_Trial_Design_Master_Protocol_synopsis_Final_18022020.pdf.
18. Vogels, C. B. F., *et al*. Analytical sensitivity and efficiency comparisons of SARS-COV-2 qRT-PCR primer-probe sets. Preprint at medRxiv https://doi.org/10.1101/2020.03.30.20048108 (2020).
19. Wyllie, A. L., *et al*. Saliva is more sensitive for SARS-CoV-2 detection in COVID-19 patients than nasopharyngeal swabs. Preprint at medRxiv https://doi.org/10.1101/2020.04.16.20067835 (2020).
20. Amanat, F. et al. A serological assay to detect SARS-CoV-2 seroconversion in humans. *Nat. Med*. **26**, 1033–1036 (2020). https://doi.org/10.1038/s41591-020-0913-5.

Acknowledgements We thank Melissa Linehan for technical and logistical assistance. This work was supported by the Women's Health Research at Yale Pilot Project Program (A.I., A.M.R.), Fast Grant from Emergent Ventures at the Mercatus Center, Mathers Foundation, the Beatrice Kleinberg Neuwirth Fund, Yale Institute for Global Health, and the Ludwig Family Foundation. IMPACT received support from the Yale COVID-19 Research Resource Fund. A.I. is an Investigator of the Howard Hughes Medical Institute. CBFV is supported by NWO Rubicon 019.181EN.004. AM is supported by NIH grant R37AI041699.

Author contributions A.I., S.B.O., A.I.K. conceived the study. C.L., P.W., J.K., J.S., T.M., J.E.O. defined parameters for flow cytometry experiments, collected and processed patient PBMC samples. P.W. acquired and analyzed the flow cytometry data. B.I., J.K., C.L., C.D.O. collected epidemiological and clinical data. F.L., A.M., J.S., E.Y.W., A.R. acquired and analyzed ELISA data. A.L.W., C.B.F.V., I.M.O., R.E., S.L., P.L., A.V., A.P., M.T. performed the virus RNA concentration assays. N.D.G. supervised virus RNA concentration assays. A.C-M., A.J.M. processed and stored patient specimens, J.B.F., C.D.C., and S.F. assisted in patient recruitment, W.L.S. supervised clinical data management, A.S. coordinated and secured funding for PBMC collection. T.T. designed the analysis scheme, analyzed, and interpreted the data for the baseline analyses. M.K.E. and S.B.O. designed the analysis scheme, and interpreted the data for the longitudinal analyses. M.K.E. analyzed the longitudinal data. T.T., M.K.E., and A.I. drafted the manuscript. A.I., A.M.R., S.B.O. revised the manuscript. A.I. secured funds and supervised the project.

Competing interests The authors declare no competing interests.

Additional information
Supplementary information is available for this paper at https://doi.org/10.1038/s41586-020-2700-3.
Correspondence and requests for materials should be addressed to A.I.
Peer review information *Nature* thanks Petter Brodin, Malik Peiris and the other, anonymous, reviewer(s) for their contribution to the peer review of this work. Peer reviewer reports are available.
Reprints and permissions information is available at http://www.nature.com/reprints.

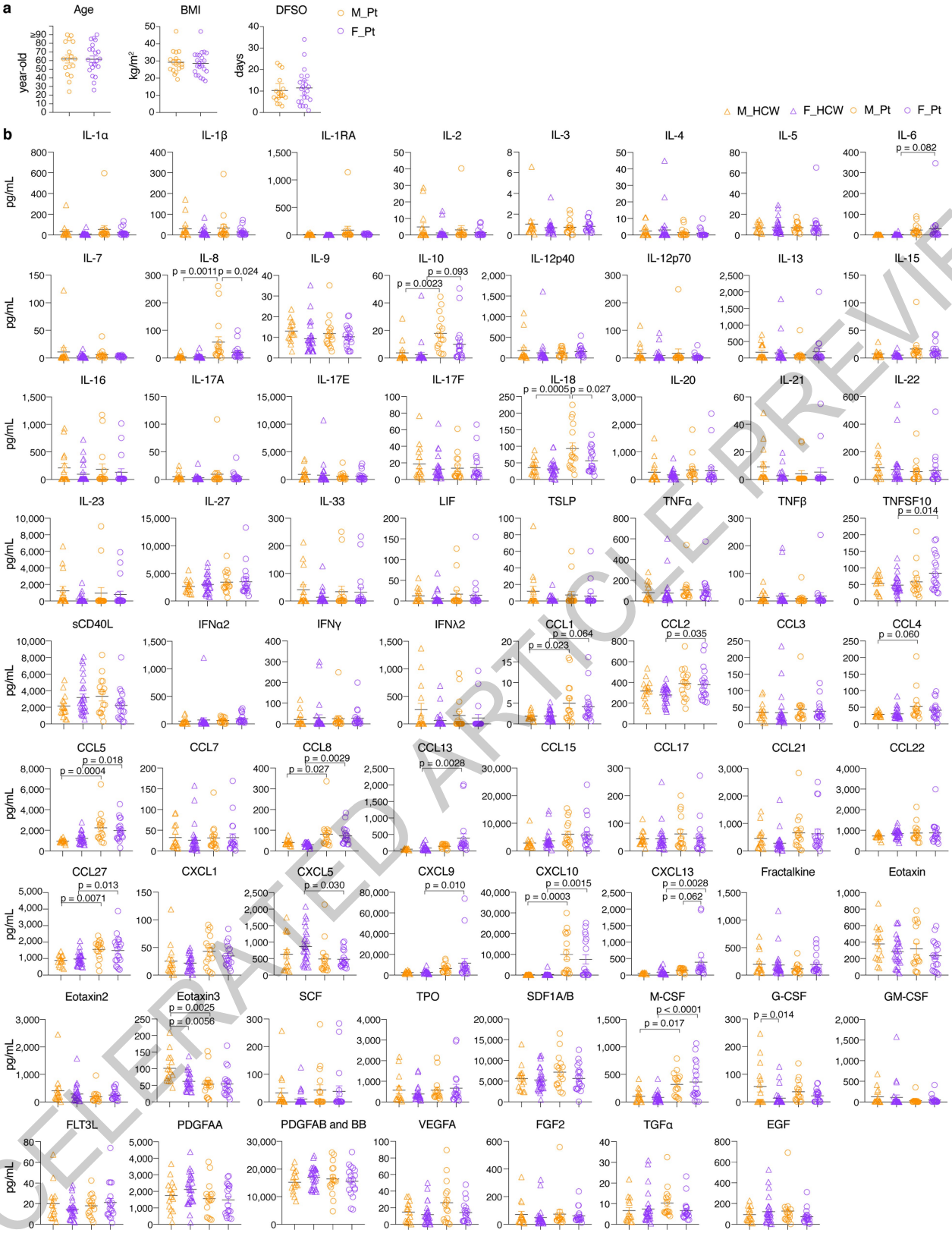

Extended Data Fig. 1 | Comparison of basic clinical parameters of Cohort A patient samples and plasma levels of 71 cytokines and chemokines at the first sampling of Cohort A. a, Comparisons of age, BMI, and DFSO at the first sampling between male and female patients in Cohort A. $n = 17$ and 22 for M_Pt and F_Pt, respectively. **b**, Comparison of the plasma levels of 71 cytokines and chemokines. $n = 15$, 28, 16, and 19 for M_HCW, F_HCW, M_Pt, and F_Pt, respectively. Data are mean ± SEM. Unpaired two-tailed *t*-test was used in **a** and one-way ANOVA with Bonferroni multiple comparison test was used for the comparisons in **b**. All p-values <0.10 are shown.

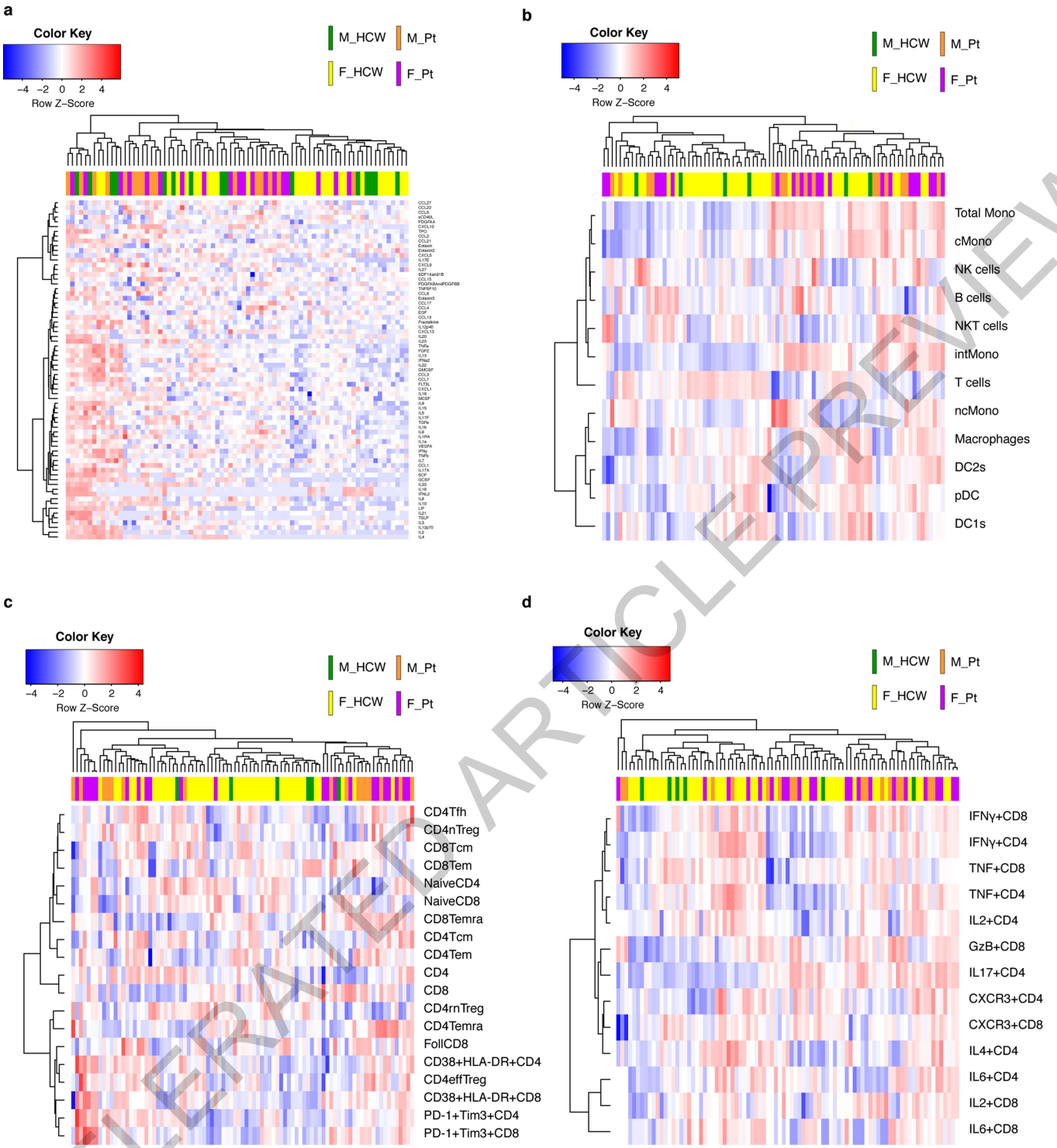

Extended Data Fig. 2 | Heatmaps of cytokines and chemokines, PBMC composition, T cell subsets, and T cell cytokine expression at the first sampling of Cohort A patients. a, A heatmap of the plasma levels (pg/mL) of 71 cytokines and chemokines. $n = 15, 28, 16$, and 19 for M_HCW, F_HCW, M_Pt, and F_Pt, respectively. **b**, A heatmap for the PBMC composition (% in live PBMCs). $n = 6, 42, 16$, and 21 for M_HCW, F_HCW, M_Pt, and F_Pt, respectively. **c**, A heatmap for the T cell subsets (% in $CD3^+$ cells). $n = 6, 45, 16$, and 22 for M_HCW, F_HCW, M_Pt, and F_Pt, respectively. **d**, A heatmap for the intracellular cytokine staining of T cells (% in $CD3^+$ cells). $n = 6, 43, 16$, and 22 for M_HCW, F_HCW, M_Pt, and F_Pt, respectively. In all of these heatmaps, log-transformed values were used for heatmap generation.

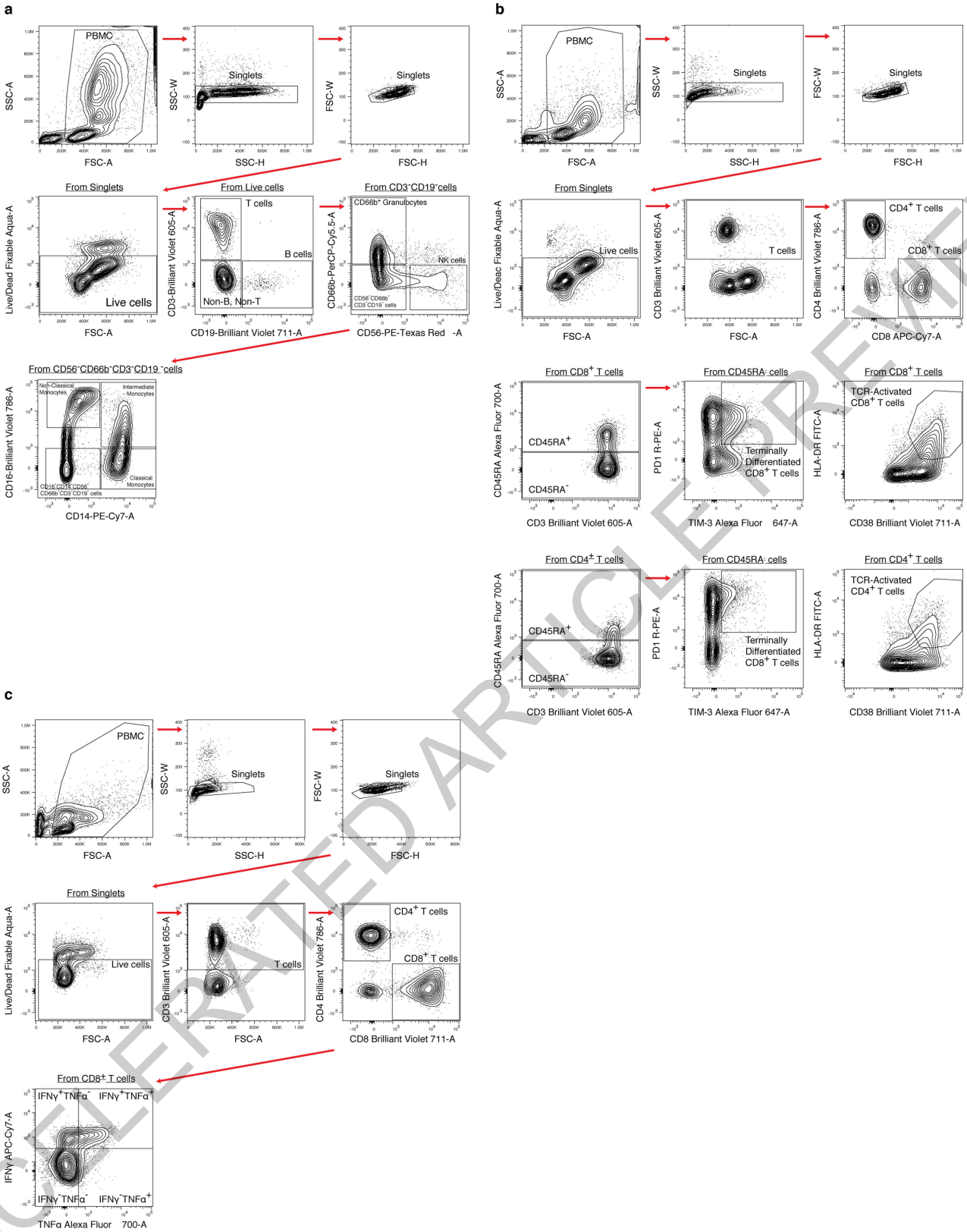

Extended Data Fig. 3 | Flow cytometry gating strategy. Gating strategy used for monocytes (**a**), CD38⁺HLA-DR⁺ and PD-1⁺TIM-3⁺ CD4/CD8 T cells (**b**), and T cell intracellular staining for IFNγ⁺ CD8 T cells (**c**).

Extended Data Table 1 | Demographic and clinical characteristics of Cohort A, Cohort B and healthcare worker comparison groups.

	Cohort A Patients (N = 39)		Cohort B Patients (N = 98)		Healthcare Workers (N = 64)		Healthcare Workers with cytokine/chemokine measurements (N = 43)		Healthcare Workers with flow cytometry (N = 51)	
	Female – N (%)	Male – N (%)	Female – N (%)	Male – N (%)	Female – N (%)	Male – N (%)	Female – N (%)	Male – N (%)	Female – N (%)	Male – N (%)
Total	22 (56.4)	17 (43.6)	51 (52.0)	47 (48.0)	45 (70.3)	19 (29.7)	28 (59.5)	15 (40.5)	45 (88.0)	6 (12.0)
Ethnicity*										
Black/African American	4 (18.2)	5 (29.4)	18 (35.3)	11 (23.4)	2 (4.4)	1 (5.3)	0 (0.0)	0 (0.0)	2 (4.6)	1 (16.7)
White	14 (63.6)	9 (52.9)	26 (51.0)	27 (57.5)	38 (84.4)	11 (57.9)	26 (100.0)	9 (60.0)	38 (84.1)	4 (66.8)
Hispanic	4 (18.2)	2 (11.8)	6 (11.8)	8 (17.0)	3 (6.7)	2 (10.5)	0 (0.0)	1 (6.7)	3 (6.8)	1 (16.7)
Other	0 (0.0)	0 (0.0)	1 (2.0)	1 (2.1)	2 (4.4)	5 (26.3)	2 (0.0)	5 (33.3)	1 (2.3)	0 (0.0)
BMI* - Mean (SD)	28.6 (6.8)	29.3 (6.6)	32.4 (9.9)	30.3 (6.0)	26.4(5.7)	28.8 (6.4)	26.4 (5.8)	31.3 (6.6)	27.4 (6.1)	28.0 (6.9)
< 18	1 (4.6)	0 (0.0)	2 (3.9)	0 (0.0)	1 (2.2)	0 (0.0)	0 (0.0)	0 (0.0)	2 (4.6)	0 (0.0)
18 – 24.9	6 (27.3)	4 (23.5)	8 (15.7)	7 (14.9)	19 (42.2)	3 (15.8)	18 (54.6)	2 (13.3)	17 (36.4)	3 (50.0)
25 – 29.9	5 (22.7)	7 (41.2)	11 (21.6)	18 (38.3)	11 (24.4)	9 (47.4)	6 (27.3)	7 (46.7)	13 (29.6)	1 (16.8)
30 – 34.9	8 (36.4)	2 (11.8)	19 (37.3)	11 (23.4)	5 (11.1)	1 (5.3)	0 (0.0)	1 (6.7)	6 (13.6)	0 (0.0)
35 +	2 (9.1)	4 (23.5)	11 (21.6)	11 (21.6)	8 (17.8)	6 (31.6)	4 (18.2)	5 (33.3)	7 (15.9)	2 (33.3)
COVID Risk Factors†										
Recent cancer treatment	3 (13.6)	1 (5.9)	3 (5.9)	4 (8.5)						
Chronic heart disease	3 (13.6)	7 (41.2)	12 (23.5)	12 (25.5)						
Hypertension	7 (31.8)	10 (58.8)	23 (45.1)	27 (57.5)						
Chronic lung disease	4 (18.2)	4 (23.5)	17 (33.3)	6 (12.8)						
Immunosuppression	3 (13.6)	1 (5.9)	4 (7.8)	1 (2.1)						
Received Tocilizumab‡			31 (60.8)	33 (64.7)						
Received Corticosteroids‡			7 (13.7)	7 (14.9)						
Admitted to the ICU‡			13 (25.5)	12 (25.5)						
Number of samples‡										
1			27 (52.9)	22 (46.8)	37 (82.2)	18 (94.7)	21 (72.7)	14 (93.3)	43 (95.5)	6 (100.0)
2			12 (23.5)	18 (38.3)	8 (17.8)	1 (5.3)	7 (27.3)	1 (6.7)	2 (4.5)	0 (0.0)
3			8 (15.7)	3 (6.4)	0 (0.0)	0 (0.0)	0 (0.0)	0 (0.0)	0 (0.0)	0 (0.0)
4			2 (3.9)	4 (8.5)	0 (0.0)	0 (0.0)	0 (0.0)	0 (0.0)	0 (0.0)	0 (0.0)
5			0 (0.0)	0 (0.0)	0 (0.0)	0 (0.0)	0 (0.0)	0 (0.0)	0 (0.0)	0 (0.0)
6			1 (2.0)	0 (0.0)	0 (0.0)	0 (0.0)	0 (0.0)	0 (0.0)	0 (0.0)	0 (0.0)
7			0 (0.0)	0 (0.0)	0 (0.0)	0 (0.0)	0 (0.0)	0 (0.0)	0 (0.0)	0 (0.0)
8			1 (2.0)	0 (0.0)	0 (0.0)	0 (0.0)	0 (0.0)	0 (0.0)	0 (0.0)	0 (0.0)
Age – mean (SD)	61.6 (17.4)	61.9 (19.5)	64.0 (16.9)	61.9 (16.7)	37.9 (11.9)	43.1 (13.2)	42.3 (12.8)	47.5 (11.2)	37.6 (11.0)	29.0 (7.6)
Days from symptom onset – mean (SD)‡	11.4 (8.1)	10.2 (6.3)	11.7 (7.2)	12.1 (7.3)						
Clinical Score – mean (SD)‡	1.3 (0.5)	1.4 (0.5)	2.5 (1.5)	2.7 (1.3)						

*Cells may not sum to total due to missing data. †Categories not mutually exclusive. ‡Gray areas indicate that data are not available or not applicable.

Extended Data Table 2 | Thirty-nine Cohort A Patient background and sample information.

ID	Sex	Age (yr-old)	Ethnicity*	BMI (kg/m^2)	COVID Risk factors†	C1‡	DFSO at C1§	Cmax‖	DFSO at the first day of Cmax¶	Deteriorated (Cmax > C1, yes=1, no=0)	Available data type#
Pt003	F	49	5	35.0	0	1	17	1		0	N, S, E, F1, F2, F3
Pt005	F	42	5	19.5	0	1	14	1		0	E, F1, F2, F3
Pt019	F	56	3	30.1	3	2	5	3	11	1	N, S, G, M, E, F1, F2, F3
Pt022	F	56	3	30.3	3,4,5	1	7	3	14	1	N, G, M, E, F1, F2, F3
Pt032	F	69	5	23.9	0	1	7	1		0	N, G, M, E, F1, F2, F3
Pt036	F	73	3	20.2	1,2,3	1	10	3	15	1	N, S, G, M, E, F1, F2, F3
Pt038	F	41	6	33.3	4	1	34	1		0	N, S, G, M, E, F1, F2, F3
Pt044	F	26	5	33.5	0	1	20	1		0	N, S, G, M, E, F1, F2, F3
Pt055	F	61	5	26.6	5	2	3	3	8	1	N, S, G, M, E, F1, F2, F3
Pt058	F	62	5	21.6	5	1	9	1		0	S, G, M, E, F1, F2, F3
Pt070	F	53	5	27.1	0	2	12	1		0	N, S, G, M, E, F1, F2, F3
Pt085	F	85	6	21.7	0	1	5	1		0	G, M, E, F1, F2, F3
Pt086	F	≥ 90	5	18.5	1	2	3	1		0	N, G, M, E, F1, F2, F3
Pt087	F	60	5	47.2	0	2	1	3	2	1	N, G, M, E, F1, F2, F3
Pt092	F	78	5	28.6	2,3	1	6	1		0	N, S, G, M, E, F1, F2, F3
Pt105	F	86	5	27.1	3	1	15	1		0	S, G, M, F1, F2, F3
Pt113	F	73	5	31.8	1,2,3	1	13	1		0	N, G, M, E, F1, F2, F3
Pt119	F	84	3	33.6	3,4	1	12	1		0	N, G, M, F1, F2, F3
Pt122	F	34	5	34.7	0	1	3	1		0	G, M, E, F1, F2, F3
Pt123	F	52	5	24.1	4	1	17	1		0	G, M, E, F1, F2, F3
Pt164	F	70	6	35.2	0	2	11	3	12	1	S, G, M, F2, F3
Pt170	F	55	6	25.2	0	1	27	1		0	S, G, M, E, F1, F2, F3
Pt004	M	62	5	27.9	0	1	21	1		0	N, S, G, M, E, F1, F2, F3
Pt007	M	44	5	25.6	3,4	1	10	1		0	N, S, G, M, E, F1, F2, F3
Pt008	M	54	5	31.5	2,3,4	1	15	1		0	E, F1, F2
Pt010	M	62	3	31.0	2,3	1	7	3	9	1	N, S, G, M, E, F1, F2, F3
Pt013	M	82	5	35.6	2,3	2	22	3	24	1	N, G, M, E, F1, F2, F3
Pt020	M	65	98	25.3	2,3	2	11	3	14	1	N, S, E, F1, F2, F3
Pt025	M	62	5	35.5	3	2	9	1		0	N, S, G, M, E, F1, F2, F3
Pt027	M	70	5	24.6	1,4	1	3	1		0	N, S, G, M, E, F3
Pt047	M	82	3	35.2	2,3	2	23	5	24	1	N, S, G, M, E, F1, F2, F3
Pt060	M	≥ 90	5	29.8	2,3	2	9	3	11	1	N, G, M, E, F1, F2, F3
Pt063	M	85	3	47.3	3	1	8	4	20	1	G, M, E, F1, F2, F3
Pt068	M	24	3	29.5	0	2	8	1		0	G, M, F1, F2, F3
Pt074	M	35	3	28.0	0	1	4	1		0	N, G, M, E, F1, F2, F3
Pt089	M	52	6	22.1	0	1	7	1		0	N, S, G, M, E, F1, F2, F3
Pt095	M	42	6	19.3	0	1	7	1		0	N, G, M, E, F1, F2, F3
Pt110	M	89	5	23.3	2,3	2	4	1		0	N, G, M, E, F1, F2, F3
Pt116	M	53	5	26.4	4,5	1	6	1		0	N, S, G, M, E, F1, F2, F3

*Ethnicity: 1 - American Indian/ Alaskan native, 2- Asian, 3- Black/ African American, 4 - Native Hawaiian/ Pacific Islander, 5 - White, 6 - Hispanic, 9 - Multiple, 98 - Unknown/ unavailable. †COVID-related risk factors: 0 - No, 1 - cancer treatment within 1 yr, 2 - chronic heart disease, 3 - hypertension, 4 - chronic lung disease (asthma, COPD, ILD), 5- immunosuppression. ‡ C1: Clinical score at the first sample collection date. § Days from symptom onset at the first sample collection. ‖ Cmax: Maximum clinical score during the admission after the first time point sample collection. ¶ Days from symptom onset at the first day Cmax was recorded in deteriorated patients. # Collected sample/data types at the first sample collection date. N; Nasopharyngeal viral load, S; Saliva viral load, G; Plasma anti-S1-IgG, M; Plasma anti-S1-IgM, E; Plasma cytokine/chemokine ELISA, F1: flow cytometry PBMC cell composition staining, F2: flow cytometry T cell surface staining, F3: flow cytometry T cell intracellular staining.

Extended Data Table 3 | Adjusted least square means difference in immune response at baseline between male and female COVID-19 patients in Cohort A and male and female healthy HCW controls.

	Female Patients vs. Male Patients*		Female Healthcare Workers vs. Male Healthcare Workers*		Female Patients vs. Female Healthcare Workers*		Male Patients vs. Male Healthcare Workers*		Difference-in-Differences*	
	Adjusted Difference (95% CI)	p-value	Adjusted Difference (95% CI)	p-value	Adjusted Difference (95% CI)	p-value	Adjusted Difference (95% CI)	p-value	Adjusted Difference (95% CI)	p-value
Antibody										
Anti-S1IgG[†]	0.08 (-0.19, 0.35)	0.87	0.01 (-0.26, 0.27)	0.99	0.31 (0.07, 0.55)	0.005	0.24 (-0.12, 0.60)	0.31	0.07 (-0.21, 0.36)	0.62
Anti-S1IgM[‡]	0.11 (-0.20, 0.41)	0.79	0.04 (-0.52, 0.61)	0.99	0.54 (0.18, 0.89)	0.001	0.47 (-0.16, 1.10)	0.20	0.06 (-0.42, 0.55)	0.79
Interferons[§]										
IFNα2	0.19 (-0.25, 0.63)	0.65	-0.14 (-0.59, 0.31)	0.84	0.48 (0.03, 0.93)	0.03	0.15 (-0.35, 0.64)	0.87	0.34 (-0.13, 0.80)	0.16
IFNγ	0.13 (-0.53, 0.78)	0.96	-0.11 (-0.78, 0.56)	0.97	0.48 (-0.19, 1.15)	0.25	0.24 (-0.50, 0.98)	0.83	0.24 (-0.45, 0.94)	0.49
IFNλ2	-0.31 (-1.17, 0.54)	0.77	-0.69 (-1.56, 0.19)	0.18	0.05 (-0.83, 0.94)	0.99	-0.32 (-1.29, 0.65)	0.82	0.37 (-0.54, 1.28)	0.42
Cytokines, Chemokines[§]										
IL-1β	-0.06 (-0.70, 0.58)	0.99	-0.36 (-1.02, 0.30)	0.48	0.21 (-0.45, 0.87)	0.84	-0.09 (-0.82, 0.63)	0.99	0.30 (-0.38, 0.98)	0.38
IL-1RA	-0.11 (-0.52, 0.30)	0.90	-0.10 (-0.52, 0.32)	0.93	0.55 (0.13, 0.97)	0.006	0.56 (0.09, 0.32)	0.01	-0.01 (-0.45, 0.43)	0.96
IL-18	-0.20 (-0.54, 0.14)	0.40	-0.13 (-0.48, 0.22)	0.76	0.30 (-0.05, 0.65)	0.11	0.38 (-0.01, 0.76)	0.06	-0.07 (-0.43, 0.29)	0.69
IL-6	-0.20 (-0.71, 0.31)	0.73	0.28 (-0.24, 0.80)	0.49	0.73 (0.21, 1.26)	0.002	1.22 (0.64, 1.79)	<0.001	-0.48 (-1.02, 0.06)	0.08
IL-8	-0.33 (-0.70, 0.04)	0.10	0.11 (-0.27, 0.48)	0.88	0.43 (0.05, 0.81)	0.02	0.87 (0.45, 1.28)	<0.001	-0.44 (-0.83, -0.04)	0.03
CXCL10	-0.45 (-0.97, 0.08)	0.13	0.15 (-0.39, 0.69)	0.89	0.76 (0.22, 1.31)	0.003	1.36 (0.76, 1.96)	<0.001	-0.60 (-1.16, -0.03)	0.04
CCL2	-0.0002 (-0.15, 0.15)	1.00	-0.02 (-0.18, 0.13)	0.98	0.07 (-0.08, 0.22)	0.60	0.05 (-0.12, 0.22)	0.88	0.02 (-0.13, 0.18)	0.76
CCL5	-0.07 (-0.25, 0.12)	0.78	0.09 (-0.10, 0.28)	0.60	0.22 (0.03, 0.41)	0.02	0.37 (0.16, 0.58)	<0.001	-0.15 (-0.35, 0.04)	0.12
M-CSF	-0.16 (-0.86, 0.54)	0.93	0.13 (-0.59, 0.85)	0.96	0.70 (-0.02, 1.42)	0.06	0.99 (0.20, 1.79)	0.008	-0.29 (-1.04, 0.45)	0.37
CCL4	-0.09 (-0.31, 0.12)	0.67	-0.03 (-0.25, 0.9)	0.98	0.06 (-0.16, 0.28)	0.90	0.12 (-0.13, 0.36)	0.58	-0.06 (-0.29, 0.17)	0.59
TNFSF10	0.18 (-0.06, 0.42)	0.21	0.002 (-0.25, 0.25)	1.00	0.15 (-0.10, 0.40)	0.38	-0.03 (-0.30, 0.25)	0.99	0.18 (-0.08, 0.44)	0.17
G-CSF	-0.29 (-1.12, 0.55)	0.80	-0.23 (-1.09, 0.62)	0.89	0.35 (-0.51, 1.21)	0.70	0.41 (-0.54, 1.35)	0.67	-0.06 (-0.94, 083)	0.90
PBMC Composition[‖]										
T Cells	3.57 (-4.78, 11.92)	0.68	2.55 (-8.54, 13.64)	0.93	-13.35 (-21.42, -5.18)	<0.001	-14.37 (-27.87, -0.86)	0.03	1.02 (-9.50, 11.54)	0.85
T Cells (10^6 cells/mL)[¶]	-0.02 (-0.48, 0.44)	0.99	0.10 (-0.39, 0.58)	0.96	-0.36 (-0.79, 0.06)	0.12	-0.25 (-0.88, 0.38)	0.73	-0.11 (-0.62, 0.39)	0.65
B Cells	-0.08 (-2.57, 2.41)	0.99	0.15 (-3.15, 3.44)	0.99	2.49 (0.06, 4.92)	0.04	2.72 (-1.30, 6.74)	0.29	-0.23 (-3.36, 2.90)	0.89
B Cells (10^6 cells/mL)[¶]	-0.01 (-0.05, 0.03)	0.94	0.01 (-0.03, 0.05)	0.92	-0.01 (-0.04, 0.03)	0.97	0.01 (-0.04, 0.06)	0.92	-0.02 (-0.06, 0.02)	0.39
Total Monocytes	-1.92 (-7.44, 3.60)	0.80	0.26 (-7.07, 7.59)	0.99	5.74 (0.33, 11.14)	0.03	7.92 (-1.02, 16.85)	0.10	-2.18 (-9.14, 4.78)	0.53
cMono	-0.83 (-4.38, 2.71)	0.93	0.001 (-4.70, 4.71)	1.00	2.01 (-1.46, 5.47)	0.43	2.84 (-2.89, 8.56)	0.56	-0.84 (-5.30, 3.63)	0.71
intMono	1.33 (-1.12, 3.77)	0.49	0.48 (-2.77, 3.73)	0.98	3.21 (0.82, 5.60)	0.004	3.26 (-1.59, 6.32)	0.40	0.85 (-2.24, 3.93)	0.59
ncMono	-2.44 (-4.47, -0.42)	0.01	-0.25 (-2.94, 2.43)	0.99	0.40 (-1.58, 2.37)	0.95	2.58 (-0.69, 5.86)	0.17	-2.19 (-4.74, 0.36)	0.09
T Cell Phenotypes[#]										
CD4	1.29 (-8.04, 10.61)	0.98	5.03 (-7.44, 17.50)	0.72	-1.80 (-10.84, 7.23)	0.95	1.94 (-13.27, 17.16)	0.99	3.74 (-15.54, 8.05)	0.53
CD8	-0.34 (-8.99, 8.30)	0.99	-1.36 (-12.91, 10.20)	0.99	2.56 (-5.81, 10.93)	0.85	1.55 (-12.55, 16.65)	0.99	1.01 (-9.91, 11.94)	0.85
CD38+HLA-DR+CD4	0.60 (-0.20, 1.39)	0.21	-0.07 (-1.14, 0.99)	0.99	0.88 (0.11, 1.66)	0.02	0.21 (-1.09, 1.51)	0.97	0.67 (-0.34, 1.68)	0.19
CD38+HLA-DR+CD8	1.03 (0.05, 2.05)	0.049	0.18 (-1.19, 1.55)	0.99	1.79 (0.80, 2.78)	<0.001	0.94 (-0.73, 2.61)	0.46	0.85 (-0.45, 2.15)	0.20
PD-1+TIM-3+CD4	0.18 (-0.36, 0.73)	0.81	-0.04 (-0.77, 0.69)	0.99	0.41 (-0.11, 0.94)	0.18	0.19 (-0.70, 1.08)	0.94	0.22 (-0.46, 0.91)	0.52
PD-1+TIM-3+CD8	0.65 (-0.11, 1.41)	0.12	-0.05 (-1.06, 0.97)	0.99	1.14 (0.41, 1.88)	<0.001	0.45 (-0.80, 0.97)	0.78	0.70 (-0.27, 1.66)	0.15

*Adjusted for age and BMI. [†]OD450; $N_{PT\_F} = 20$, $N_{Pt\_M} = 15$, $N_{HCW\_F} = 74$, $N_{HCW\_M} = 13$. [‡]OD450; $N_{PT\_F} = 20$, $N_{Pt\_M} = 15$, $N_{HCW\_F} = 18$, $N_{HCW\_M} = 3$. [§]Log_{10} pg/mL; $N_{PT\_F} = 19$, $N_{Pt\_M} = 16$, $N_{HCW\_F} = 28$, $N_{HCW\_M} = 15$. [‖]As percent of live cells, unless otherwise indicated; $N_{PT\_F} = 21$, $N_{Pt\_M} = 16$, $N_{HCW\_F} = 51$, $N_{HCW\_M} = 6$. [¶]$N_{PT\_F} = 33$, $N_{Pt\_M} = 40$, $N_{HCW\_F} = 51$, $N_{HCW\_M} = 6$. [#]As percent of CD3-positive cells; $N_{PT\_F} = 21$, $N_{Pt\_M} = 16$, $N_{HCW\_F} = 51$, $N_{HCW\_M} = 6$. P-values determined using two-sided *t*-test with Tukey correction for multiple pairwise comparisons.

Extended Data Table 4 | Adjusted least square means difference over time in immune response between male and female COVID-19 patients in Cohort B.

	Female Patients vs. Male Patients*	
	Adjusted Difference (95% CI)	p-value
Viral Load[†]		
Nasopharyngeal	0.18 (-0.58, 0.94)	0.63
Saliva	-0.15 (-1.19, 0.90)	0.78
Antibody[‡]		
Anti-S1IgG	-0.06 (-0.30, 0.18)	0.63
Anti-S1IgM	0.02 (-0.16, 0.19)	0.86
Interferon Response[§]		
IFNα2	0.25 (0.04, 0.47)	0.02
IFNγ	0.21 (-0.04, 0.46)	0.10
IFNλ2	-0.18 (-0.55, 0.20)	0.35
Cytokines, Chemokines and Growth Factors[§]		
IL-1β	-0.03 (-0.33, 0.26)	0.82
IL-1RA	-0.11 (-0.36, 0.14)	0.39
IL-18	-0.003 (-0.25, 0.24)	0.98
IL-6	0.07 (-0.17, 0.30)	0.58
IL-8	-0.08 (-0.26, 0.11)	0.44
CXCL10	-0.18 (-0.50, 0.13)	0.25
CCL2	-0.02 (-0.11, 0.06)	0.57
CCL5	-0.12 (-0.22, -0.02)	0.02
M-CSF	0.001 (-0.27, 0.27)	0.99
CCL4	-0.07 (-0.18, 0.04)	0.19
TNFSF10	0.08 (-0.05, 0.20)	0.22
G-CSF	-0.14 (-0.47, 0.20)	0.43
PBMC Composition[‖]		
T Cells	6.12 (0.49, 11.76)	0.03
T Cells (10^6 cells/mL)[¶]	0.13 (0.01, 0.25)	0.04
B Cells	-0.66 (-2.24, 0.92)	0.41
B Cells (10^6 cells/mL)[¶]	0.02 (-0.02, 0.05)	0.33
Total Monocytes	-2.32 (-6.56, 1.92)	0.28
cMono	-1.31 (-3.38, 0.76)	0.21
intMono	0.27 (-0.78, 1.33)	0.61
ncMono	-1.36 (-4.59, 1.87)	0.41
T Cell Phenotypes[#]		
CD4	-1.02 (-7.45, 5.41)	0.75
CD8	3.62 (-1.62, 8.86)	0.17
CD38+HLA-DR+CD4	-0.09 (-0.62, 0.44)	0.74
CD38+HLA-DR+CD8	0.71 (-0.31, 1.73)	0.17
PD-1+TIM-3+CD4	0.06 (-0.22, 0.34)	0.67
PD-1+TIM-3+CD8	0.36 (-0.21, 0.93)	0.21

*Adjusted for age, BMI, days from symptom onset, Toci treatment, CS treatment and ICU status. [†]Log_{10}(SARS-CoV-2 copies/mL); Nasopharyngeal $N_{PT\_F} = 33$, $N_{Pt\_M} = 30$; Saliva $N_{PT\_F} = 20$, $N_{Pt\_M} = 18$. [‡]OD450; $N_{PT\_F} = 44$, $N_{Pt\_M} = 39$. [§]Log_{10} pg/mL; $N_{PT\_F} = 48$, $N_{Pt\_M} = 43$. [‖]As percent of live cells, unless indicated otherwise; $N_{PT\_F} = 46$, $N_{Pt\_M} = 42$. [¶]$N_{PT\_F} = 33$, $N_{Pt\_M} = 40$. [#]As percent of CD3-positive cells; $N_{PT\_F} = 49$, $N_{Pt\_M} = 42$. P-values determined using two-sided *t*-test and Morel-Bokossa-Neerchal correction.

Extended Data Table 5 | Adjusted least square means difference over time in immune response between male and female COVID-19 patients in Cohort B and male and female healthy HCW controls.

	Female Patients vs. Male Patients*		Female Healthcare Workers vs. Male Healthcare Workers*		Female Patients vs. Female Healthcare Workers*		Male Patients vs. Male Healthcare Workers*		Difference-in-Differences*	
	Adjusted Difference (95% CI)	p-value	Adjusted Difference (95% CI)	p-value	Adjusted Difference (95% CI)	p-value	Adjusted Difference (95% CI)	p-value	Adjusted Difference (95% CI)	p-value
Antibody										
Anti-S1IgG[†]	-0.10 (-0.41, 0.22)	0.86	-0.0001 (-0.13, 0.13)	1.00	0.56 (0.23, 0.89)	<0.001	0.66 (0.28, 1.03)	<0.001	-0.10 (-0.35, 0.16)	0.46
Anti-S1IgM[‡]	0.01 (-0.23, 0.24)	0.99	0.04 (-0.13, 0.22)	0.92	0.72 (0.43, 1.02)	<0.001	0.76 (0.42, 1.10)	<0.001	-0.04 (-0.26, 0.18)	0.74
Interferons[§]										
IFNα2	0.26 (0.004, 0.52)	0.046	-0.14 (-0.57, 0.28)	0.82	0.50 (0.12, 0.89)	0.01	0.10 (-0.32, 0.52)	0.93	0.41 (0.02, 0.79)	0.04
IFNγ	0.19 (-0.14, 0.51)	0.45	-0.07 (-0.74, 0.61)	0.99	0.64 (0.13, 1.15)	0.01	0.39 (-0.22, 1.00)	0.35	0.25 (-0.32, 0.82)	0.39
IFNλ2	-0.19 (-0.65, 0.27)	0.71	-0.58 (-1.45, 0.29)	0.31	-0.09 (-0.78, 0.60)	0.99	-0.48 (-1.36, 0.40)	0.50	0.39 (-0.38, 1.15)	0.32
Cytokines, Chemokines[§]										
IL-1β	-0.07 (-0.41, 0.28)	0.96	-0.27 (-0.94, 0.40)	0.73	0.23 (-0.27, 0.73)	0.63	0.03 (-0.58, 0.63)	0.99	0.20 (-0.38, 0.79)	0.50
IL-1RA	-0.05 (-0.36, 0.26)	0.98	-0.09 (-0.52, 0.35)	0.96	0.65 (0.27, 1.03)	<0.001	0.61 (0.21, 1.02)	<0.001	0.04 (-0.40, 0.47)	0.87
IL-18	-0.02 (-0.32, 0.29)	0.99	-0.22 (-0.65, 0.22)	0.58	0.49 (0.03, 0.96)	0.04	0.29 (-0.14, 0.72)	0.30	0.20 (-0.22, 0.62)	0.35
IL-6	-0.10 (-0.59, 0.39)	0.96	0.16 (-0.34, 0.66)	0.83	1.70 (1.11, 2.28)	<0.001	1.96 (1.44, 2.48)	<0.001	-0.26 (-0.80, 0.28)	0.34
IL-8	-0.08 (-0.32, 0.16)	0.84	0.18 (-0.16, 0.52)	0.53	0.70 (0.38, 1.02)	<0.001	0.96 (0.65, 1.26)	<0.001	-0.25 (-0.58, 0.08)	0.13
CXCL10	-0.22 (-0.63, 0.18)	0.48	0.12 (-0.17, 0.41)	0.72	1.05 (0.56, 1.55)	<0.001	1.40 (1.04, 1.75)	<0.001	-0.34 (-0.75, 0.07)	0.10
CCL2	-0.03 (-0.14, 0.08)	0.91	-0.03 (-0.16, 0.11)	0.96	0.09 (-0.02, 0.21)	0.17	0.10 (-0.06, 0.25)	0.38	-0.003 (-0.13, 0.13)	0.96
CCL5	-0.11 (-0.23, 0.01)	0.08	0.07 (-0.04, 0.18)	0.34	0.11 (-0.03, 0.24)	0.19	0.29 (0.17, 0.40)	<0.001	-0.18 (-0.30, -0.06)	0.005
M-CSF	0.01 (-0.33, 0.36)	0.99	0.19 (-0.66, 1.04)	0.94	0.68 (0.07, 1.29)	0.02	0.86 (0.08, 1.63)	0.02	-0.18 (-0.88, 0.52)	0.62
CCL4	-0.08 (-0.22, 0.07)	0.50	0.02 (-0.11, 0.15)	0.98	0.14 (-0.06, 0.33)	0.26	0.23 (0.11, 0.36)	<0.001	-0.10 (-0.26, 0.06)	0.22
TNFSF10	0.09 (-0.10, 0.28)	0.62	-0.06 (-0.30, 0.17)	0.90	0.18 (-0.05, 0.40)	0.18	0.03 (-0.24, 0.29)	0.99	0.15 (-0.08, 0.38)	0.20
G-CSF	-0.15 (-0.59, 0.29)	0.80	-0.41 (-1.36, 0.55)	0.69	0.64 (0.01, 1.26)	0.045	0.39 (-0.51, 1.28)	0.68	0.25 (-0.56, 1.06)	0.54
PBMC Composition[‖]										
T Cells	6.42 (-1.52, 14.36)	0.16	1.99 (-5.38, 9.36)	0.90	-17.66 (-27.00, -8.32)	<0.001	-22.1 (-32.90, -11.28)	<0.001	4.43 (-3.77, 12.63)	0.29
T Cells (10^6 cells/mL)[¶]	0.11 (-0.04, 0.25)	0.21	0.10 (-0.32, 0.52)	0.93	-0.30 (-0.59, -0.02)	0.03	-0.32 (-0.73, 0.10)	0.21	-0.01 (-0.32, 0.35)	0.95
B Cells	-0.85 (-2.85, 1.16)	0.70	0.39 (-1.55, 2.33)	0.96	3.86 (1.81, 5.91)	<0.001	5.09 (2.08, 8.10)	<0.001	-1.23 (-3.37, 0.91)	0.26
B Cells (10^6 cells/mL)[¶]	0.01 (-0.02, 0.04)	0.95	0.01 (-0.02, 0.05)	0.72	0.03 (-0.01, 0.07)	0.33	0.03 (-0.01, 0.07)	0.15	-0.001 (-0.04, 0.03)	0.75
Total Monocytes	-3.19 (-8.66, 2.29)	0.44	0.14 (-4.88, 5.16)	0.99	6.38 (-0.05, 12.81)	0.05	9.70 (1.78, 17.62)	0.009	-3.32 (-8.83, 2.18)	0.24
cMono	-1.35 (-3.78, 1.09)	0.48	0.08 (-2.53, 2.70)	0.99	2.32 (-0.68, 5.32)	0.19	3.75 (0.11, 7.39)	0.04	-1.43 (-4.08, 1.22)	0.29
intMono	0.45 (-0.84, 1.73)	0.81	0.61 (-0.64, 1.85)	0.59	1.85 (-0.03, 3.72)	0.06	2.01 (0.40, 3.62)	0.008	-0.16 (-1.52, 1.20)	0.82
ncMono	-2.24 (-6.81, 2.33)	0.58	-0.56 (-3.87, 9.72)	0.97	2.15 (-2.64, 6.95)	0.65	3.84 (-2.05, 9.72)	0.33	-1.68 (-5.75, 2.39)	0.42
T Cell Phenotypes[#]										
CD4	-1.14 (-9.07, 6.79)	0.98	4.72 (-7.96, 17.39)	0.77	-1.54 (-9.46, 6.39)	0.96	4.32 (-9.68, 18.32)	0.86	-5.86 (-17.26, 5.55)	0.31
CD8	3.21 (-3.23, 9.66)	0.57	-0.59 (-6.86, 5.67)	0.99	3.65 (-3.06, 10.37)	0.49	-0.15 (-8.71, 8.41)	1.00	3.81 (-3.23, 10.85)	0.29
CD38+HLA-DR+CD4	-0.19 (-0.90, 0.52)	0.90	-0.14 (-0.53, 0.25)	0.79	1.09 (0.38, 1.80)	<0.001	1.14 (0.36, 1.92)	0.001	-0.05 (-0.67, 0.56)	0.87
CD38+HLA-DR+CD8	0.62 (-0.58, 1.81)	0.54	0.23 (-0.33, 0.80)	0.71	2.25 (0.58, 3.92)	0.003	0.86 (0.48, 3.24)	0.003	0.39 (-0.54, 1.31)	0.41
PD-1+TIM-3+CD4	0.02 (-0.38, 0.42)	0.99	-0.01 (-0.42, 0.40)	0.99	0.59 (0.16, 1.02)	0.003	0.57 (-0.07, 1.20)	0.10	0.03 (-0.42, 0.47)	0.90
PD-1+TIM-3+CD8	0.32 (-0.39, 1.02)	0.65	-0.003 (-0.32, 0.31)	1.00	1.31 (0.54, 2.09)	<0.001	0.99 (0.21, 1.77)	0.006	0.32 (-0.27, 0.91)	0.29

*Adjusted for age and BMI. [†]OD450; $N_{PT\_F} = 44$, $N_{Pt\_M} = 39$, $N_{HCW\_F} = 74$, $N_{HCW\_M} = 13$. [‡]OD450; $N_{PT\_F} = 44$, $N_{Pt\_M} = 39$, $N_{HCW\_F} = 18$, $N_{HCW\_M} = 3$. [§]Log_{10} pg/mL; $N_{PT\_F} = 48$, $N_{Pt\_M} = 43$, $N_{HCW\_F} = 28$, $N_{HCW\_M} = 15$. [‖]As percent of live cells, unless otherwise indicated; $N_{PT\_F} = 46$, $N_{Pt\_M} = 42$, $N_{HCW\_F} = 51$, $N_{HCW\_M} = 6$. [¶]$N_{PT\_F} = 33$, $N_{Pt\_M} = 40$, $N_{HCW\_F} = 51$, $N_{HCW\_M} = 6$. [#]As percent of CD3-positive cells; $N_{PT\_F} = 49$, $N_{Pt\_M} = 42$, $N_{HCW\_F} = 51$, $N_{HCW\_M} = 6$. P-values were determined using two-sided *t*-test with Tukey correction for multiple pairwise comparisons.

Extended Data Table 6 | Adjusted least square means difference between male and female COVID-19 patients in Cohort A by patient trajectory.

	Female Deteriorated vs. Male Deteriorated*		Female Stable vs. Male Stable*		Female Deteriorated vs. Female Stable*		Male Deteriorated vs. Male Stable*		Difference-in-Differences*	
	Adjusted Difference (95% CI)	p-value	Adjusted Difference (95% CI)	p-value	Adjusted Difference (95% CI)	p-value	Adjusted Difference (95% CI)	p-value	Adjusted Difference (95% CI)	p-value
PBMC Composition										
ncMono[2]	-4.22 (-10.68, 2.24)	0.30	-1.91 (-6.20, 2.39)	0.63	-1.02 (-6.14, 4.10)	0.95	1.30 (-4.82, 7.42)	0.94	-2.32 (-8.51, 3.89)	0.45
CD38+HLA-DR+CD4	1.72 (-0.73, 4.17)	0.25	0.27 (-1.32, 1.86)	0.97	0.80 (-1.13, 2.74)	0.68	-0.65 (-2.92, 1.63)	0.87	1.45 (-0.89, 3.79)	0.22
CD38+HLA-DR+CD8	2.23 (-1.01, 5.46)	0.26	0.39 (-1.71, 2.50)	0.96	0.45 (-2.10, 3.01)	0.96	-1.38 (-4.39, 1.63)	0.60	1.84 (-1.26, 4.93)	0.24
PD-1+TIM-3+CD4	1.20 (-0.44, 2.85)	0.22	-0.15 (-1.22, 0.92)	0.98	0.74 (-0.56, 2.04)	0.42	-0.61 (-2.14, 0.92)	0.70	1.35 (-0.22, 2.92)	0.09
PD-1+TIM-3+CD8	0.80 (-1.70, 3.30)	0.82	0.67 (-0.96, 2.30)	0.68	-0.40 (-2.38, 1.58)	0.95	-0.53 (-2.86, 1.79)	0.93	0.13 (-2.26, 2.52)	0.91
IFNγ-CD8	5.92 (-1.23, 13.08)	0.13	-0.92 (-5.76, 3.92)	0.95	3.51 (-2.16, 9.17)	0.35	-3.33 (-10.12, 3.46)	0.55	6.84 (-0.12, 13.80)	0.05
Cytokines, Chemokines[§]										
IL-8	-0.22 (-1.20, 0.77)	0.93	-0.31 (-0.93, 0.31)	0.53	-0.22 (-1.02, 0.57)	0.87	-0.31 (-1.18, 0.56)	0.76	0.09 (-0.83, 1.01)	0.84
IL-18	-0.28 (-0.84, 0.28)	0.52	-0.15 (-0.51, 0.20)	0.64	0.05 (-0.40, 0.51)	0.99	0.18 (-0.32, 0.68)	0.75	-0.13 (-0.66, 0.39)	0.61
CXCL10	-0.14 (-1.56, 1.29)	0.99	-0.57 (-1.46, 0.31)	0.31	0.92 (-0.23, 2.07)	0.15	0.48 (-0.78, 1.73)	0.73	0.44 (-0.88, 1.76)	0.50
sCD40L	-0.11 (-0.76, 0.54)	0.97	-0.29 (-0.69, 0.12)	0.24	-0.47 (-0.99, 0.06)	0.09	-0.65 (-1.22, -0.07)	0.02	0.18 (-0.42, 0.78)	0.55
CCL5	0.07 (-0.36, 0.51)	0.97	-0.16 (-0.43, 0.12)	0.41	0.39 (0.03, 0.74)	0.03	0.16 (-0.23, 0.54)	0.70	0.23 (-0.18, 0.64)	0.25
TNFSF10	0.51 (-0.02, 1.05)	0.06	0.05 (-0.29, 0.38)	0.98	0.35 (-0.08, 0.79)	0.14	-0.12 (-0.59, 0.36)	0.91	0.47 (-0.03, 0.97)	0.07
MCSF	0.001 (-1.02, 1.03)	1.00	-0.16 (-0.80, 0.48)	0.51	0.56 (-0.26, 1.39)	0.27	0.41 (-0.50, 1.31)	0.62	0.16 (-0.79, 1.11)	0.73
IL-15	0.33 (-0.30, 0.95)	0.50	-0.17 (-0.56, 0.22)	0.64	0.34 (-0.17, 0.85)	0.28	-0.16 (-0.71, 0.40)	0.87	0.50 (-0.09, 1.08)	0.09

*Adjusted for age and days from symptom onset. [†]As percent of CD3-positive cells unless otherwise indicated. $N_{F\_DETERIORATED} = 6$, $N_{M\_DETERIORATED} = 6$, $N_{F\_STABILIZED} = 16$, $N_{M\_}STABILIZED = 11$. [‡]As percent of live cells. [§]Log_{10} pg/mL. P-values determined using two-sided *t*-test with Tukey correction for multiple comparisons.

Extended Data Table 7 | Definitions of each cell subset in flow cytometry with specific markers.

	Cell population	Definition by markers
Flow cytometry staining panels	**Live singlet gate**	**PBMC/Single Cells/Single Cells/Live…**
1: PBMC cell composition staining	B cells	…/CD19+CD3-
	T cells	…/CD19-CD3+
	NKT cells	…/CD19-CD3+/CD3+CD56+
	NK cells	…/CD19-CD3-/CD56+CD66b-
	Classical Monocytes (cMono)	…/CD19-CD3-/CD56-CD66b-/CD14+CD16-
	Intermediate Monocytes (intMono)	…/CD19-CD3-/CD56-CD66b-/CD14+CD16var
	Non-Classical Monocytes (ncMono)	…/CD19-CD3-/CD56-CD66b-/CD14-CD16+
	Plasmacytoid DCs (pDC)	…/CD19-CD3-/CD56-CD66b-/CD14-CD16-/CD304+
	Macrophages	…/CD19-CD3-/CD56-CD66b-/CD14-CD16-/CD304-/CD11b+
	DC1	…/CD19-CD3-/CD56-CD66b-/CD14-CD16-/CD304-/CD141+HLA-DR+
	DC2	…/CD19-CD3-/CD56-CD66b-/CD14-CD16-/CD304-/CD1c+HLA-DR+
2: T cell subsets staining (by surface markers)	CD8 T cells	…/CD3+/CD8+CD4-
	Naïve CD8T	…/CD3+/CD8+CD4-/CD3+CD45RA+/CD127+CCR7+/CD3+PD1-
	Temra CD8T	…/CD3+/CD8+CD4-/CD3+CD45RA+/CD127-CCR7-
	Central Memory CD8T (CD8Tcm)	…/CD3+/CD8+CD4-/CD3+CD45RA-/CD127+CCR7+
	Effector Memory CD8T (CD8Tem)	…/CD3+/CD8+CD4-/CD3+CD45RA-/CD127+CCR7-
	Terminally Differentiated CD8T (PD-1+TIM-3+CD8)	…/CD3+/CD8+CD4-/CD3+CD45RA-/TIM3+PD1+
	Follicular CD8T (FollCD8)	…/CD3+/CD8+CD4-/CD3+CD45RA-/CXCR5+PD1+
	TCR-activated CD8T (CD38+HLA-DR+CD8)	…/CD3+/CD8+CD4-/CD38+HLA-DR+
	CD4 T cells	…/CD3+/CD8-CD4+
	Naïve CD4T	…/CD3+/CD8-CD4+/CD3+CD45RA+/CD127+CCR7+/CD3+PD1-
	Temra CD4T	…/CD3+/CD8-CD4+/CD3+CD45RA+/CD127-CCR7-
	Resting Natural Regulatory CD4T (CD4rn Treg)	…/CD3+/CD8-CD4+/CD3+CD45RA+/CD127-CD25hi/CD3+HLA-DR-
	Central Memory CD4T (CD4Tcm)	…/CD3+/CD8-CD4+/CD3+CD45RA-/CD127+CCR7+
	Effector Memory CD4T (CD4Tem)	…/CD3+/CD8-CD4+/CD3+CD45RA-/CD127+CCR7-
	Terminally Differentiated CD4T (PD-1+TIM-3+CD4)	…/CD3+/CD8-CD4+/CD3+CD45RA-/TIM3+PD1+
	Effector Regulatory CD4T (CD4effTreg)	…/CD3+/CD8-CD4+/CD3+CD45RA-/CD127-CD25hi Treg/CD3+HLA-DR+
	Natural Regulatory CD4T (CD4n Treg)	…/CD3+/CD8-CD4+/CD3+CD45RA-/CD127-CD25hi Treg/CD3+HLA-DR-
	TCR-activated CD4T (CD38+HLA-DR+CD4)	…/CD3+/CD8-CD4+/CD38+HLA-DR+
3: Cytokine producing T cells staining (intracellular staining)	Granzyme B-expressing CD8T	…/CD3+/CD8+CD4-/GranzymeB+
	IFNy- expressing CD8T	…/CD3+/CD8+CD4-/IFNy+
	TNFa-expressing CD8T	…/CD3+/CD8+CD4-/TNFa+
	IL2- expressing CD8T	…/CD3+/CD8+CD4-/IL2+
	IL6-expressing CD8T	…/CD3+/CD8+CD4-/IL6+
	CXCR3-expressing CD8T	…/CD3+/CD8+CD4-/CXCR3+
	IFNy- expressing CD4T	…/CD3+/CD8-CD4+/IFNy+
	TNFa-expressing CD4T	…/CD3+/CD8-CD4+/TNFa+
	IL2- expressing CD4T	…/CD3+/CD8-CD4+/IL2+
	IL6-expressing CD4T	…/CD3+/CD8-CD4+/IL6+
	IL4-expressing CD4T	…/CD3+/CD8-CD4+/IL4+
	IL17-expressing CD4T	…/CD3+/CD8-CD4+/IL17+
	CXCR3-expressing CD4T	…/CD3+/CD8-CD4+/CD3+CXCR3+

nature research

Corresponding author(s): Akiko Iwasaki

Last updated by author(s): August 11, 2020

Reporting Summary

Nature Research wishes to improve the reproducibility of the work that we publish. This form provides structure for consistency and transparency in reporting. For further information on Nature Research policies, see our Editorial Policies and the Editorial Policy Checklist.

Statistics

For all statistical analyses, confirm that the following items are present in the figure legend, table legend, main text, or Methods section.

n/a	Confirmed	
☐	☒	The exact sample size (*n*) for each experimental group/condition, given as a discrete number and unit of measurement
☐	☒	A statement on whether measurements were taken from distinct samples or whether the same sample was measured repeatedly
☐	☒	The statistical test(s) used AND whether they are one- or two-sided *Only common tests should be described solely by name; describe more complex techniques in the Methods section.*
☐	☒	A description of all covariates tested
☐	☒	A description of any assumptions or corrections, such as tests of normality and adjustment for multiple comparisons
☐	☒	A full description of the statistical parameters including central tendency (e.g. means) or other basic estimates (e.g. regression coefficient) AND variation (e.g. standard deviation) or associated estimates of uncertainty (e.g. confidence intervals)
☐	☒	For null hypothesis testing, the test statistic (e.g. *F*, *t*, *r*) with confidence intervals, effect sizes, degrees of freedom and *P* value noted *Give P values as exact values whenever suitable.*
☒	☐	For Bayesian analysis, information on the choice of priors and Markov chain Monte Carlo settings
☐	☒	For hierarchical and complex designs, identification of the appropriate level for tests and full reporting of outcomes
☐	☒	Estimates of effect sizes (e.g. Cohen's *d*, Pearson's *r*), indicating how they were calculated

Our web collection on statistics for biologists contains articles on many of the points above.

Software and code

Policy information about availability of computer code

Data collection	EPIC EHR software (retrospective EMR review and clinical data aggregation) and REDCap 9.3.6 (clinical data aggregation).
Data analysis	R (version 3.6.3), ggplot2 (version 3.3.0), Graphpad Prism (version 8), SAS (version 9.4), Attune NxT (version 3.1.2), FlowJo (version 10.6, Tree Star).

For manuscripts utilizing custom algorithms or software that are central to the research but not yet described in published literature, software must be made available to editors and reviewers. We strongly encourage code deposition in a community repository (e.g. GitHub). See the Nature Research guidelines for submitting code & software for further information.

Data

Policy information about availability of data

All manuscripts must include a data availability statement. This statement should provide the following information, where applicable:

- Accession codes, unique identifiers, or web links for publicly available datasets
- A list of figures that have associated raw data
- A description of any restrictions on data availability

All the flow cytometry data will be available via ImmPort website (study ID: SDY1648). All the data (viral load, antibody titer, ELISA data) used to generate figures and tables in this study are included in the Supplementary Information Table 1.

Field-specific reporting

Please select the one below that is the best fit for your research. If you are not sure, read the appropriate sections before making your selection.

☒ Life sciences ☐ Behavioural & social sciences ☐ Ecological, evolutionary & environmental sciences

For a reference copy of the document with all sections, see nature.com/documents/nr-reporting-summary-flat.pdf

Life sciences study design

All studies must disclose on these points even when the disclosure is negative.

Sample size	No statistical methods were used to calculate the sample size. Sample size was determined based on the number of patients admitted to Yale-New Haven Hospital (YNHH) between March 18th and May 9th that were enrolled and consented with the current study under IRB and HIC approved protocol #2000027690. Patients were identified though screening of EMR records for potential enrollment. Individuals with active chemotherapy against cancers, pregnant patients, patients with background hematological abnormalities, patients with autoimmune diseases (e.g. rheumatoid arthritis), and patients with a history of organ transplantation and on immunosuppressive agents were not included, and in total 98 patients were included in this study. Informed consent was obtained by trained staff and sample collection commenced immediately upon study enrollment. Clinical specimens were collected approximately every 4 days where an individual's clinical status permitted, and was continued until patient discharge or expiration.
Data exclusions	Two extreme outlier samples for cytokine ELISA in the entire study. Measurements from these individuals were outliers (beyond 1.5x the interquartile range) in more than half of the cytokines measured. This strongly suggested that a technical error occurred during these two experiments or poor sample quality. Likewise, for flow cytometry, data on myeloid panel and T cell surface staining panel for two individuals were outliers in more than half of the parameters measured, which suggested the poor staining quality during the experiments. Thus, data of these samples were excluded from the analyses.
Replication	The measurements were not replicated - longitudinal analyses of samples from human individuals.
Randomization	This is not relevant as this is an observational study.
Blinding	At the time of sample acquisition and processing, scientists were completely unaware of the patients' conditions. Blood acquisition is performed and recorded by a separate team. Information of patients' conditions are not available until after processing and analysing raw data by flow cytometry and ELISA. A clinical team, separate from the experimental team, performs chart review to determine patients' relevant statistics. Cytokines and facs analyses were blinded. Patients clinical information and clinical scores coding were only revealed after data collection.

Reporting for specific materials, systems and methods

We require information from authors about some types of materials, experimental systems and methods used in many studies. Here, indicate whether each material, system or method listed is relevant to your study. If you are not sure if a list item applies to your research, read the appropriate section before selecting a response.

Materials & experimental systems

n/a	Involved in the study
☐	☒ Antibodies
☒	☐ Eukaryotic cell lines
☒	☐ Palaeontology and archaeology
☒	☐ Animals and other organisms
☐	☒ Human research participants
☒	☐ Clinical data
☒	☐ Dual use research of concern

Methods

n/a	Involved in the study
☒	☐ ChIP-seq
☐	☒ Flow cytometry
☒	☐ MRI-based neuroimaging

Antibodies

Antibodies used	All antibodies used in this study are against human proteins. BB515 anti-hHLA-DR (G46-6) (1:400) (BD Biosciences), BV785 antihCD16 (3G8) (1:100) (BioLegend), PE-Cy7 anti-hCD14 (HCD14) (1:300) (BioLegend), BV605 anti-hCD3 (UCHT1) (1:300) (BioLegend), BV711 anti-hCD19 (SJ25C1) (1:300) (BD Biosciences), AlexaFluor647 anti-hCD1c (L161) (1:150) (BioLegend), Biotin anti-hCD141 (M80) (1:150) (BioLegend), PE-Dazzle594 anti-hCD56 (HCD56) (1:300) (BioLegend), PE anti-hCD304 (12C2) (1:300) (BioLegend), APCFire750 anti-hCD11b (ICRF44) (1:100) (BioLegend), PerCP/Cy5.5 anti-hCD66b (G10F5) (1:200) (BD Biosciences), BV785 anti-hCD4 (SK3) (1:200) (BioLegend), APCFire750 or PE-Cy7 or BV711 anti-hCD8 (SK1) (1:200) (BioLegend), BV421 anti-hCCR7 (G043H7) (1:50) (BioLegend), AlexaFluor 700 anti-hCD45RA (HI100) (1:200) (BD Biosciences), PE anti-hPD1 (EH12.2H7) (1:200) (BioLegend), APC anti-hTIM3 (F38-2E2) (1:50) (BioLegend), BV711 anti-hCD38 (HIT2) (1:200) (BioLegend), BB700 anti-hCXCR5 (RF8B2) (1:50) (BD Biosciences), PECy7 anti-hCD127 (HIL-7R-M21) (1:50) (BioLegend), PE-CF594 anti-hCD25 (BC96) (1:200) (BD Biosciences), BV711 anti-hCD127

(HIL-7R-M21) (1:50) (BD Biosciences), BV421 anti-hIL17a (N49-653) (1:100) (BD Biosciences), AlexaFluor 700 anti-hTNFa (MAb11) (1:100) (BioLegend), PE or APC/Fire750 anti-hIFNy (4S.B3) (1:60) (BioLegend), FITC anti-hGranzymeB (GB11) (1:200) (BioLegend), AlexaFluor 647 anti-hIL-4 (8D4-8) (1:100) (BioLegend), BB700 anti-hCD183/CXCR3 (1C6/CXCR3) (1:100) (BD Biosciences), PE-Cy7 antihIL-6 (MQ2-13A5) (1:50) (BioLegend), PE anti-hIL-2 (5344.111) (1:50) (BD Biosciences), BV785 anti-hCD19 (SJ25C1) (1:300) (BioLegend), BV421 anti-hCD138 (MI15) (1:300) (BioLegend), AlexaFluor700 anti-hCD20 (2H7) (1:200) (BioLegend), AlexaFluor 647 anti-hCD27 (M-T271) (1:350) (BioLegend), PE/Dazzle594 anti-hIgD (IA6-2) (1:400) (BioLegend), PE-Cy7 anti-hCD86 (IT2.2) (1:100) (BioLegend), APC/Fire750 anti-hIgM (MHM-88) (1:250) (BioLegend), BV605 anti-hCD24 (ML5) (1:200) (BioLegend), BV421 anti-hCD10 (HI10a) (1:200) (BioLegend), BV421 anti-CDh15 (SSEA-1) (1:200) (BioLegend), AlexaFluor 700 Streptavidin (1:300) (ThermoFisher), BV605 Streptavidin (1:300) (BioLegend).

Validation

All antibodies used in this study are commercially available, and all have been validated by the manufacturers and used by other publications. Likewise, we titrated these antibodies according to our own our staining conditions. The following were validated in the following species: BB515 anti-hHLA-DR (G46-6) (BD Biosciences) (Human, Rhesus, Cynomolgus, Baboon), BV785 anti-hCD16 (3G8) (BioLegend) (Human, African Green, Baboon, Capuchin Monkey, Chimpanzee, Cynomolgus, Marmoset, Pigtailed Macaque, Rhesus, Sooty Mangabey, Squirrel Monkey), PE-Cy7 anti-hCD14 (HCD14) (BioLegend) (Human), BV605 anti-hCD3 (UCHT1) (BioLegend) (Human, Chimpanzee), BV711 anti-hCD19 (SJ25C1) (BD Biosciences) (Human), AlexaFluor647 anti-hCD1c (L161) (BioLegend) (Human, African Green, Baboon, Cynomolgus, Rhesus), Biotin anti-hCD141 (M80) (BioLegend) (Human, African Green, Baboon), PE-Dazzle594 anti-hCD56 (HCD56) (BioLegend) (Human, African Green, Baboon, Cynomolgus, Rhesus), PE anti-hCD304 (12C2) (BioLegend) (Human), APCFire750 anti-hCD11b (ICRF44) (BioLegend) (Human, African Green, Baboon, Chimpanzee, Common Marmoset, Cynomolgus, Rhesus, Swine), PerCP/Cy5.5 anti-hCD66b (G10F5) (BD Biosciences) (Human), BV785 anti-hCD4 (SK3) (BioLegend) (Human), APCFire750 or PE-Cy7 or BV711 anti-hCD8 (SK1) (BioLegend) (Human, Cross-Reactivity: African Green, Chimpanzee, Cynomolgus, Pigtailed Macaque, Rhesus, Sooty Mangabey), BV421 anti-hCCR7 (G043H7) (BioLegend) (Human, African Green, Baboon, Cynomolgus, Rhesus), AlexaFluor 700 anti-hCD45RA (HI100) (BD Biosciences) (Human), PE anti-hPD1 (EH12.2H7) (BioLegend) (Human, African Green, Baboon, Chimpanzee, Common Marmoset, Cynomolgus, Rhesus, Squirrel Monkey), APC antihTIM3 (F38-2E2) (BioLegend) (Human), BV711 anti-hCD38 (HIT2) (BioLegend) (Human, Chimpanzee, Horse), BB700 anti-hCXCR5 (RF8B2) (BD Biosciences) (Human), PE-Cy7 anti-hCD127 (HIL-7R-M21) (BioLegend) (Human), PE-CF594 anti-hCD25 (BC96) (BD Biosciences) (Human, Rhesus, Cynomolgus, Baboon), BV711 anti-hCD127 (HIL-7R-M21) (BD Biosciences) (Human), BV421 anti-hIL-17a (N49-653) (BD Biosciences) (Human), AlexaFluor 700 anti-hTNFa (MAb11) (BioLegend) (Human, Cat, Cross-Reactivity: Chimpanzee, Baboon, Cynomolgus, Rhesus, Pigtailed Macaque, Sooty Mangabey, Swine), PE or APC/Fire750 anti-hIFNy (4S.B3) (BioLegend) (Human, Cross-Reactivity: Chimpanzee, Baboon, Cynomolgus, Rhesus), FITC anti-hGranzymeB (GB11) (BioLegend) (Human, Mouse, Cross-Reactivity: Rat), AlexaFluor 647 anti-hIL-4 (8D4-8) (BioLegend) (Human, Cross-Reactivity: Chimpanzee, Baboon, Cynomolgus, Rhesus), BB700 anti-hCD183/CXCR3 (1C6/CXCR3) (BD Biosciences) (Human, Rhesus, Cynomolgus, Baboon), PE-Cy7 anti-IL-6 (MQ2-13A5) (BioLegend) (Human), PE anti-hIL-2 (5344.111) (BD Biosciences) (Human), BV785 anti-hCD19 (SJ25C1) (BioLegend) (Human), BV421 anti-hCD138 (MI15) (BioLegend) (Human), AlexaFluor700 anti-hCD20 (2H7) (BioLegend) (Human, Baboon, Capuchin Monkey, Chimpanzee, Cynomolgus, Pigtailed Macaque, Rhesus, Squirrel Monkey), AlexaFluor 647 anti-hCD27 (M-T271) (BioLegend) (Human, Cross-Reacitivity: Baboon, Cynomolgus, Rhesus), PE/Dazzle594 anti-hIgD (IA6-2) (BioLegend) (Human), PE-Cy7 anti-hCD86 (IT2.2) (BioLegend) (Human, African Green, Baboon, Capuchin Monkey, Common Marmoset, Cotton-topped Tamarin, Chimpanzee, Cynomolgus, Rhesus), APC/Fire750 anti-hIgM (MHM-88) (BioLegend) (Human, African Green, Baboon, Cynomolgus, Rhesus), BV605 anti-hCD24 (ML5) (BioLegend) (Human, Cross-Reactivity: Chimpanzee), BV421 anti-hCD10 (HI10a) (BioLegend) (Human, African Green, Baboon, Capuchin monkey, Chimpanzee, Cynomolgus, Rhesus), BV421 anti-hCD15 (SSEA-1) (BioLegend) (Human), AlexaFluor 700 Streptavidin (1:300) (ThermoFisher), BV605 Streptavidin (1:300) (BioLegend).

Human research participants

Policy information about studies involving human research participants

Population characteristics	Fifty-one female (age 64.0±16.9) and 47 male (age 61.9±16.7) patients were included. The detailed demographic information can be found in Extended Data Table 1.
Recruitment	Patients admitted to the Yale New Haven Hospital (YNHH) between the 18th of March through the 9th of May 2020, were recruited to the Yale IMPACT study (Implementing Medical and Public Health Action Against Coronavirus CT) after testing positive for SARS-CoV2 by qRT-PCR. (serology was further confirmed for all patients enrolled). Patients were identified though screening of EMR records for potential enrollment with no self selection. Informed consent was obtained by trained staff and sample collection commenced immediately upon study enrollment. Clinical specimens were collected approximately every 4 days where an individual's clinical status permitted, and was continued until patient discharge or expiration.
Ethics oversight	Yale Human Research Protection Program Institutional Review Boards. Informed consents were obtained from all enrolled patients and healthcare workers. • Our research protocol was reviewed and approved by the Yale School of Medicine IRB and HIC (#2000027690). Informed consent was obtained by trained staff and records maintained in our research database for the duration of our study. There were no minors included on this study.

Note that full information on the approval of the study protocol must also be provided in the manuscript.

Flow Cytometry

Plots

Confirm that:

☒ The axis labels state the marker and fluorochrome used (e.g. CD4-FITC).

☒ The axis scales are clearly visible. Include numbers along axes only for bottom left plot of group (a 'group' is an analysis of identical markers).

☒ All plots are contour plots with outliers or pseudocolor plots.

☒ A numerical value for number of cells or percentage (with statistics) is provided.

Methodology

Sample preparation	Freshly isolated PBMCs were stained for live and dead markers, blocked with Human TruStan FcX , stained for surface markers and then fixed with PFA 4%. For intracellular cytokine staining following stimulation , cells were surface stained, washed and fixed in 4% PFA. After permeabilization with 1X Permeabilization Buffer cells were stained for intracellular cytokines analysis.
Instrument	Cells were acquired on an Attune NXT (ThermoFisher).
Software	Data were analysed using FlowJo software version 10.6 software (Tree Star).
Cell population abundance	Cell population abundance: Cells populations were reported in various formats including as a number or concentration of the patient's blood sample (x106cells/mL), as a proportion of live, single PBMC (% of Live), or as a proportion of a parent gate (% of CD4 T cells, % of Monocytes, etc.). The full gating path for clarification is included in the extended figures.
Gating strategy	SSC-A and FSC-A parameters were used to select leukocytes from isolated PBMCs. Live and dead cells were defined based on aqua staining. Singlets were separated based on SSC/ FSC parameters. Leukocytes were gated based on to identify lymphocytes (CD3/CD4/CD8/CD19/CD56 markers), granulocytes (CD16,CD14, HLA-DR markers) and pDCs, and cDCs (CD304, CD1c, CD141). TCR-activated T cells, Terminally-differentiated T cells, and additional subsets.were defined using HLA-DR, CD38, CCR7,CD127, PD1, TIM-3, CXCR5, CD45RA, CD25. Intracellular T cell gating strategy to identify CD4 and/or CD8 T cells secreting TNFa, IFN-y, IL-6, IL-2, GranzymeB, IL-4, and/or IL-17 were defined using the specif markers: CD3, CD4, CD8, TNF, IFN, IL-6, IL-2, IL-4, IL-17 and granzyme B.

☒ Tick this box to confirm that a figure exemplifying the gating strategy is provided in the Supplementary Information.